

AD-768 598

COMPARISON OF ION BEAM PROBE AND
LANGMUIR PROBE DIAGNOSTIC TECHNIQUES

John C. Glowienka

Rensselaer Polytechnic Institute

Prepared for:

Air Force Office of Scientific Research

July 1973

DISTRIBUTED BY:

NTIS

National Technical Information Service
U. S. DEPARTMENT OF COMMERCE
5285 Port Royal Road, Springfield Va. 22151

AFOSR -TR -73 -1632

COMPARISON OF ION BEAM PROBE AND LANGMUIR PROBE
DIAGNOSTIC TECHNIQUES

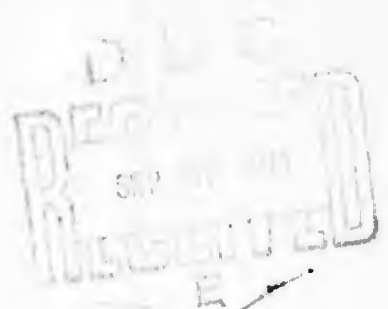
by

John C. Glowienka

RPDL Report No. 73-2

July 1973

This research was supported by the Air Force Office of Scientific
Research (AFSC) under Grant No. 72-2191



PLASMA DYNAMICS LABORATORY
Rensselaer Polytechnic Institute
Troy, N. Y. 12181

Approved for public release; distribution unlimited

Conditions of Reproduction

Reproduction, translation, publication, use and disposal in whole
or in part by or for the United States Government is permitted.

Reproduced by
NATIONAL TECHNICAL
INFORMATION SERVICE
U.S. Department of Commerce
Springfield, MA 01104

UNCLASSIFIED

Security Classification

DOCUMENT CONTROL DATA - R & D

(Starting with the citation of title, body of abstract and indexing annotation must be entered when the overall report is classified)

SPONSORING MILITARY ACTIVITY (Corporate authors)

RENSSELAER POLYTECHNIC INSTITUTE
ELECTROPHYSICS AND ELECTRONIC ENGINEERING DIVISION
TROY, NEW YORK 12181

12. REPORT SECURITY CLASSIFICATION

UNCLASSIFIED

13. GROUP

1. REPORT TITLE

COMPARISON OF ION BEAM PROBE AND LANGMUIR PROBE DIAGNOSTIC TECHNIQUES

4. DESCRIPTIVE NOTES (Type of report and inclusive dates)

Scientific Interim

3. AUTHOR(S) (Last name, middle initial, first name)

JOHN C. SLOWIENKA

5. REPORT DATE

JULY 1973

7a. TOTAL NO. OF PAGES

96

7b. NO. OF REFS

26

6. CONTRACT OR GRANT NO.

AFOSR-72-2191

8. ORIGINATOR'S REPORT NUMBER(S)

RPL 73-2

9. PROJECT NO.

9752-01

10. OTHER REPORT NO(S) (Any other numbers that may be assigned this report)

AFOSR - 1R - 73 - 1632

c. 61102F

d. 681308

10. DISTRIBUTION STATEMENT

Approved for public release; distribution unlimited

11. SUPPLEMENTARY NOTES

TECH, OTHER

12. SPONSORING MILITARY ACTIVITY

AF Office of Scientific Research (NAE)
1400 Wilson Boulevard
Arlington, Virginia 22209

13. ABSTRACT

This thesis concerns the comparison of two diagnostic techniques for magnetically confined plasmas - the Langmuir Probe technique and the Ion Beam Probe technique. The comparison is made for plasma charged particle number density and plasma electron temperature measurements on the Rensselaer Hollow Cathode Discharge. The principles, theory, and system description required to understand and operate each probe are discussed. Experimental results taken with each device on the same plasma are given and compared. It is found that one or both techniques need to be extended for a more valid comparison. Work towards a more sensitive Ion Beam Probe is mentioned with this comparison in mind. In addition, the application of the Ion Beam Probe to a study of a plasma with a coherent instability and the feedback stabilization of the instability is discussed.

DD FORM 1473

UNCLASSIFIED

Security Classification

KEY WORDS

LINK A

LINK B

LINK C

ROLE

WT

ROLE

WT

ROLE

WT

THERMONUCLEAR FUSION

MAGNETICALLY CONFINED PLASMAS

PLASMA DIAGNOSTICS

CHARGED PARTICLE NUMBER DENSITY

SPACE POTENTIAL

TEMPERATURE

CURRENT DENSITY

LANGMUIR PROBE

ION BEAM PROBE

ia

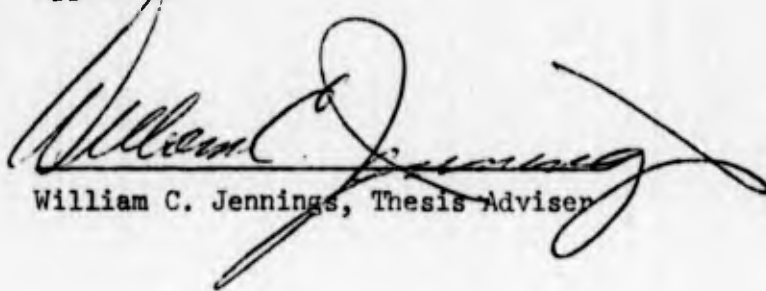
COMPARISON OF ION BEAM PROBE AND
LANGMUIR PROBE DIAGNOSTIC TECHNIQUES

by

John C. Glowienka

A Thesis Submitted to the Graduate
Faculty of Rensselaer Polytechnic Institute
in Partial Fulfillment of the
Requirements for the Degree of
MASTER OF SCIENCE

Approved:



William C. Jennings, Thesis Adviser

Rensselaer Polytechnic Institute
Troy, New York

May 1973

••
//

TABLE OF CONTENTS

	Page
LIST OF FIGURES.....	v
ACKNOWLEDGEMENT.....	vii
ABSTRACT.....	viii
I. INTRODUCTION.....	1
A. Motivation for Thesis.....	1
B. Justification of New Diagnostics.....	1
C. Types of Measurements.....	2
D. Contents of Thesis.....	3
II. LANGMUIR PROBING.....	4
A. Principles of Langmuir Probing.....	4
B. Langmuir Probe Theory.....	6
C. System Description for Langmuir Probe.....	12
III. ION BEAM PROBING.....	17
A. Principles.....	17
1. Physics.....	17
2. Application.....	20
3. Measurements.....	23
B. IBP Theory of Density and Temperature Measurement.....	25
C. System Description of the IBP.....	27
1. Ion Source.....	29
a. Ion Gun.....	29
i. Ion Supply.....	29
ii. Optics.....	35
iii. Deflection and Steering.....	39
iv. Physical Support.....	39
b. Environmental Support.....	42
c. Electronics.....	45
2. Detectors.....	49
a. Types.....	49
b. Environmental Protection.....	51
c. Electronics.....	54

	Page
IV. EXPERIMENTAL RESULTS.....	57
A. Langmuir Probe Data.....	57
B. Ion Beam Probe Data.....	61
V. DISCUSSION.....	66
VI. FUTURE CONSIDERATIONS.....	70
A. Slaving System.....	70
B. Electrostatic Energy Analyzer.....	71
C. Future Investigations.....	73
LITERATURE CITED.....	74
APPENDICES.....	76

LIST OF FIGURES

	Page
Figure 1 Langmuir Probe Diagnostics.....	5
Figure 2 Langmuir Probe Plots.....	7
Figure 3 Langmuir Probe.....	13
Figure 4 Bellows Assembly.....	14
Figure 5 Monitoring Module.....	15
Figure 6 Beam Probing System.....	18
Figure 7 Detection Grid.....	21
Figure 8 Beam Probe Measurements.....	24
Figure 9 Plot of $f(T_e)_1/f(T_e)_2$ for Potassium and Sodium...	28
Figure 10 Source Preparation.....	31
Figure 11 Ion Source Tester.....	34
Figure 12 Ion Source Catalog Form.....	36
Figure 13 Ion Gun.....	38
Figure 14 Deflection (Sweep and Steering).....	40
Figure 15 Support Cradle.....	43
Figure 16 Ion Gun Differential Pumping System.....	46
Figure 17 Sweep Amplifiers.....	48
Figure 18 Detector (R^{++} ions enter from the right).....	53
Figure 19 D.C. Amplifier.....	55
Figure 20 Langmuir Probe Electron Temperature T_e Versus Distance R From Arc Center. Arc is Helium.....	59
Figure 21 Langmuir Probe Number Density n Versus Distance From Arc Center. Arc is Helium.....	60
Figure 22 Isometric $nf(T_e)$ for Potassium Ions in a Helium Arc.....	62

		Page
Figure 23	Raw IBP Data I_s/I_p for Potassium and Sodium in Helium.....	63
Figure 24	Number Density n and Electron Temperature T_e for a Helium Arc.....	65
Figure 25	Number Density n as Obtained by the IBP and Langmuir Probe in a Helium Arc.....	67
Figure 26	Electron Temperature T_e as Obtained from an IBP and a Langmuir Probe in a Helium Arc.....	68
Figure 27	Slaving System.....	72
Figure 28	RPI Plasma Machine.....	77

ACKNOWLEDGEMENT

I would like to express my thanks and appreciation to my advisor Dr. William C. Jennings for the time, patience, and encouragement he has given me throughout this work. I would also like to thank Dr. Robert L. Hickok for his technical advice and for the opportunity to work under him. Last but not least, I would like to warmly thank my comrade in arms, Doctor-to-be, Robert Reinovsky. Although we worked together, we both know who the leader of the group is.

ABSTRACT

This thesis concerns the comparison of two diagnostic techniques for magnetically confined plasmas - the Langmuir Probe technique and the Ion Beam Probe technique. The comparison is made for plasma charged particle number density and plasma electron temperature measurements on the Rensselaer Hollow Cathode Discharge.

The principles, theory, and system description required to understand and operate each probe are discussed. Experimental results taken with each device on the same plasma are given and compared. It is found that one or both techniques need to be extended for a more valid comparison. Work towards a more sensitive Ion Beam Probe is mentioned with this comparison in mind. In addition, the application of the Ion Beam Probe to a study of a plasma with a coherent instability and the feedback stabilization of the instability is discussed.

I. INTRODUCTION

A. Motivation for Thesis

The motivation for this thesis is to compare a new diagnostic technique for magnetically confined plasmas, ion beam probing, with the work horse of plasma diagnostics, the Langmuir probe. The comparison is done by measuring two types of plasma parameters, charged particle number density and plasma electron temperature with each technique.

B. Justification of New Diagnostics

One extensive area of plasma research is the development of controlled thermonuclear fusion. This development is one approach to the solution of the energy crisis. There are two major thrusts-- magnetically confined plasma machines and inertially confined plasma machines. This discussion is limited to magnetically confined devices. The constituents of the fusion reaction are ionized Deuterium and Tritium in a hot gaseous plasma. They are brought together via collision, fuse, and give off energy. It must be emphasized that the goal of this research is not merely to understand a laboratory curiosity, rather the goal is to develop an efficient source of power. With this in mind, there are three conditions that must be satisfied for such a power cycle. The plasma must be hot enough; it must be dense enough, and the constituents must remain in a specified volume long enough for the fusion reaction to take place to such an extent for the economic question to be satisfied. In essence, it is desired

to build a small star. A look at these requirements has been done by Lawson. The fusion reaction requires an ignition temperature of 100 million degrees Kelvin.

The particle count and existence time product must be at least 10^{14} sec/cc. This is the Lawson or $n\tau$ criterion. So far, power cycle fusion has not occurred because present fusion devices are at least an order of magnitude short on all counts. To resolve the questions raised by this failure and to improve the fusion machines, comprehensive research is being conducted at many levels. From this research one point has arisen: there is a definite need for a detailed knowledge of the plasma, i.e. what is happening at every point in the plasma at any time.

C. Types of Measurement

Ideally, this detailed knowledge would include the density and velocity of all plasma constituents as continuous functions of space and time. This is impossible. A compromise that yields sufficient information is measurement of charged particle density, n , electron and ion temperature, T_e and T_i , space potential, ϕ , current density, J_z , along the confining field. The question of actual measurement can be divided with two categories--passive and active measurement. In passive measurement, information about the plasma is obtained from what the plasma emits, radiation and particles. This is unsatisfactory because the plasma masks the detailed knowledge by macroscopic phenomena. In the active approach, the plasma

is probed; measuring devices are brought to it and information is obtained from plasma response.

There are many techniques for measuring plasma parameters;¹ however, most are unsatisfactory because they fail to give measurements that are continuous functions of space and time for many of the desired parameters. The workhorse of plasma diagnostics has been the Langmuir probe. It can measure n , T_e , and ϕ as continuous functions of space and time. However, as the plasma temperature rises, their use decreases; they are useless in fusion plasmas for measuring the desired parameters because they are destroyed by the heat. The new technique, Ion Beam Probing (IBP), can measure all four parameters as continuous functions of space and time.^{2,3,4,5} The technique is unique in that all probing and detecting is initiated away from the hostile plasma environment. All that is required is a knowledge of the magnetic confining field.

D. Contents of Thesis

Each diagnostic technique will be discussed with heavy emphasis placed on the description of the IBP system. Each system will be described in terms of basic principles and physics, the necessary theory for n and T_e , and the hardware. Use of both systems will be covered. Data and results from both techniques will be given and compared. Finally, a brief section will be devoted to future considerations.

II. LANGMUIR PROBING

A. Principles of Langmuir Probing

Langmuir Probing is a sampling of energetic plasma particles by means of a small electrode biased with respect to some reference. The reference can be ground or a larger electrode situated in the plasma such as the anode or cathode. Data taken with Langmuir probes on the Rensselaer HCD (see Appendix A), is referenced to the anode which is ground. See Figure 1. At a fixed bias, particles of higher energy will tend to approach the probe more often than lower energy particles, regardless of charge. Consequently, it can easily be seen that there are several regimes of operation of the probe. Consider a plasma with two constituents, electrons and positive ions, each with their own energy distributions; this is not far from reality in most plasma systems since the plasma is formed by stripping an electron away from an atom or molecule. Referring to Figure 2a, when the probe is strongly negative, the electrode or probe repels all electrons and collects only ions (I). Moving toward positive bias, there will be a region (II) where very high energy electrons can penetrate the probe's repelling field and start subtracting from the ion current. Moving further on, there will be a point where electron current exactly equals the ion current, hence zero total current. This is the floating potential V_f . Moving higher in bias voltage, more and more electrons are collected as well as fewer ions (III). Eventually a point is reached where there is no field between the plasma and the probe; the plasma potential or space potential ϕ

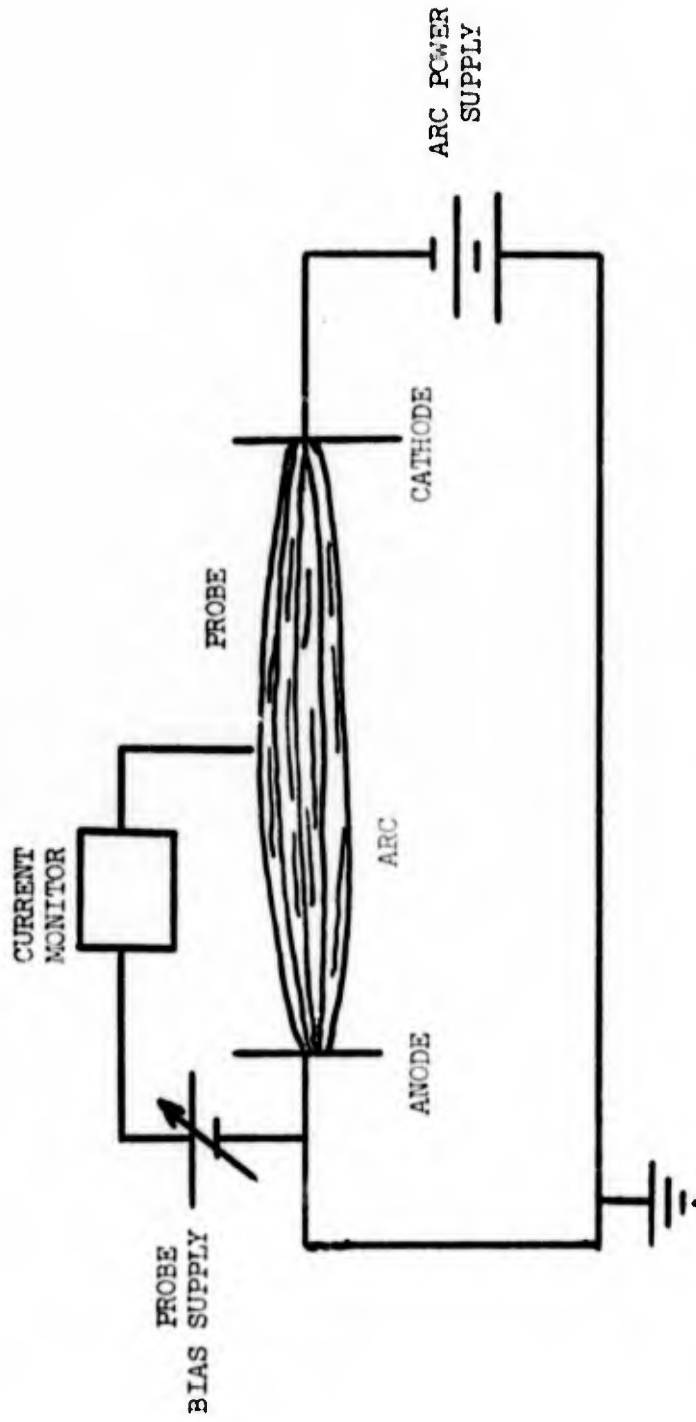
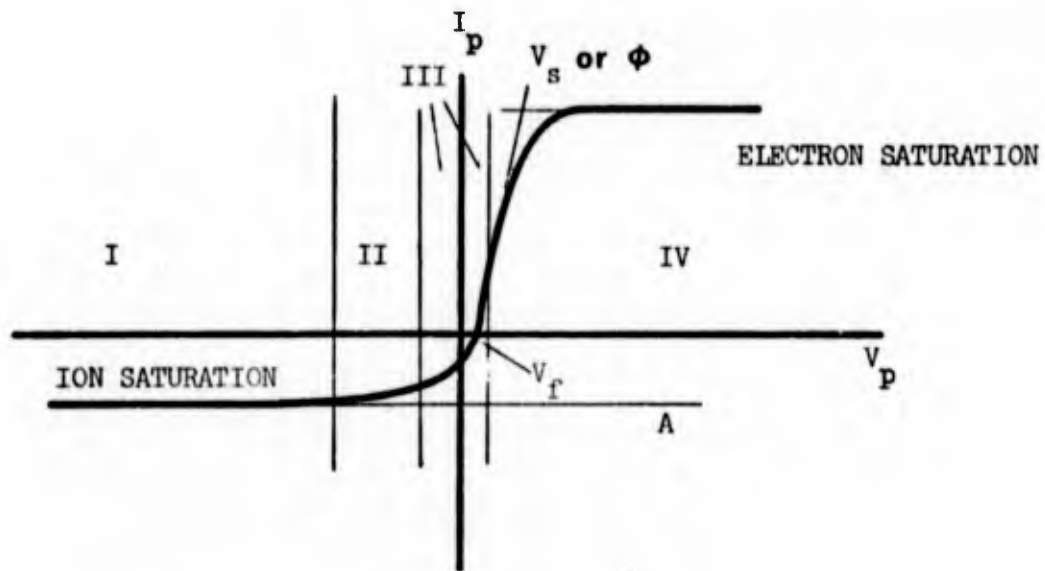


Figure 1 Langmuir Probe Diagnostics

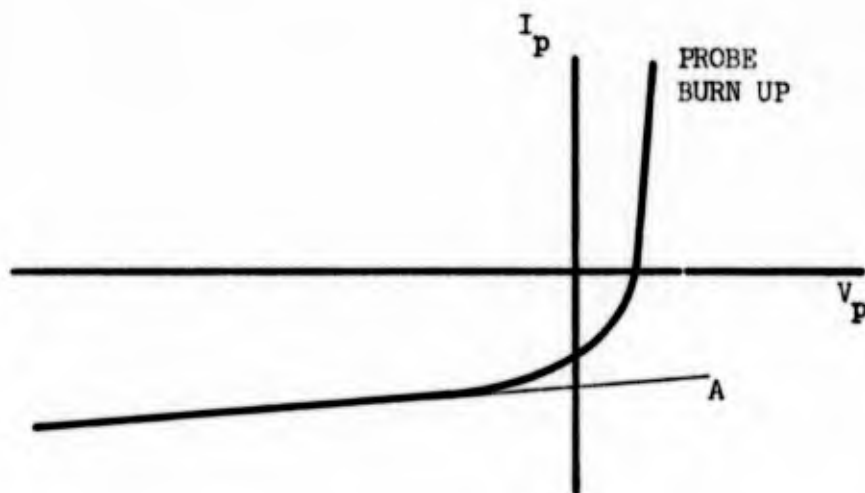
equals the probe potential. At this point, particles are collected according to their thermal velocities. Electrons move much faster than ions because they have a much smaller mass; the current is predominantly electron current. Any further positive biasing accelerates the electrons to the probe, and the ion component will quickly vanish. By further increasing the bias, the electron current saturates (IV) as was the case for the ions in region I. It should be noted that electron saturation may not be obtained in hot dense plasmas because high currents will burn up the probe. In addition, the point of space potential may not be reached for the same region. In most glow discharges both the space potential and electron saturation will be reached. In hotter and denser plasmas such as magnetically confined arc plasmas, space potential and electron saturation may only be obtained in regions away from the core of the plasma. A typical Langmuir probe plot close to the core of the Rensselaer HCD is given in Figure 2b. From plots like 2a or 2b, plasma charged particle density and electron temperature can be obtained. The Langmuir probe plot contains the information about the plasma. The unfolding of this data into useful information will be described in the Theory and Result Section.

B. Langmuir Probe Theory

The principles of Langmuir probes are quite simple and straightforward. The theory is not so simple; in several cases of interest, the theory is intractable and incomplete, e.g. magnetically confined plasmas. This is not to say that there is a lack of theories



a Typical Langmuir Probe Plot with
Electron Current Positive



b Probe Close to Core or High Positive Bias,
Electron Current Burns Up Probe

Figure 2 Langmuir Probe Plots

as the literature will attest. Huddlestone and Leonard's⁷ text is a good starting point for literature search on Langmuir probes. In essence, there are two types of probe theories: direct and inverse.⁸ The predominant one is the direct; this is the creation of the theorist. Plasma parameters and operating statistics are arbitrarily chosen to create a plasma, and a theory or plasma model is created. The results are generally a set of non-dimensionalized current-voltage plots that describe plasma behavior. For that particular plasma, the plots represent the theoretical response; the plasma may not exist however.

The inverse problem is the one that confronts the experimentalist. By varying bias voltages and monitoring current, a description of local plasma parameters is obtained but locked in the plot. The inverse problem is to unravel the information. Inverse methods generally exist for more simple, less interesting plasmas.⁹ As mentioned earlier, the problem enters when the plasma is hot, dense, and magnetically confined. There exist only incomplete solutions for this area.

One of the basic assumptions made of probe theories is that the probe does not disturb the plasma. From a first order look, this could possibly be the case. A plasma tends to shield itself from any external charge or boundary within a dimension called a Debye length, λ_D . This is a characteristic of the plasma that depends on the number of charged particles present and their average energy. If this length and the probe radius, a , were small with respect to the characteristic dimension of the plasma, it is possible for the probe not to disturb

the plasma. When a magnetic field is introduced an anisotropy is created which does not allow the shielding to take place. The particles cannot move to positions where the redistribution takes place because they cannot cross the magnetic field lines. Along the magnetic field lines, the redistribution takes place for shielding, but across the magnetic confining field, the electric field of the probe extends out into the plasma and perturbs the plasma. Another complication arises from collisions. If the plasma has collision effects that dominate all the way to the probe surface, particle velocity distributions are uncertain leaving the problem incomplete. Difficulties enter the theory when certain physical parameters dominate in size over other parameters as listed below:

When

1. The probe radius, a , is large
2. The mean free path between electron neutral collisions λ is small compared to probe radius or shield length
3. The ion Larmor radius r_i is small compared to λ

For the first entry, simply, if the probe is larger it will perturb the plasma. The second has to do with establishing a Maxwellian distribution for repelled particles. If there is a collision dominated regime within the sheath, the distribution is no longer Maxwellian at the sheath edge. It is from this Maxwellian sheath that information about the plasma is contained. The third involves the anisotropy due to the particles being unable to cross field lines and reestablish sheath conditions. It can be shown that if this situation did not

exist, the theory reduces to the theories of Bohm, Burhop, and Massey¹⁰ and Langmuir¹¹, where to within 20%

$$I_{ion} = 0.4 A_p \left(\frac{kT_e}{m_{ion}} \right)^{1/2} n_o \quad (1)$$

$$I_e = A_p n_o \left(\frac{kT_e}{2\pi m_e} \right)^{1/2} \exp - \frac{eV_p}{kT_e} \quad (2)$$

where I_{ion} is the ion saturation current (region I Figure 2a)
 I_e is the electron current (region II and III Figure 2a)
 A_p is the surface area of the probe
 k is Boltzmann's constant
 T_e is the electron temperature of a Maxwellian distribution of electrons
 n_o is the charge particle number density
 m_i is the ion mass
 m_e is the electron mass
 V_p is the probe bias potential with respect to a plasma reference

Equation 1 applies to ion saturation (region I on Figure 2a).

The probe voltage is strongly negative and accelerates the ions to high velocities. Since this occurs in a magnetic field, the Larmor radius increases with increasing accelerating probe voltage. There will be a voltage where the ion Larmor radius exceeds the mean free path. The anisotropy across the field is eliminated. The particles are still collision dominated but at characteristic lengths larger

than λ . In addition, according to the Bohm criterion¹², the colder species, the ions, have a distinct minimum velocity as they cross the sheath. The minimum velocity is a function of the electron temperature and is much greater than the ion drift velocity. Consequently, in ion saturation the current is insensitive to ion temperature.

Equation 2 applies to the transition region (II and III on Figure 2a) and again depends on λ being the dominant length. With λ large, the distribution of the electrons at the sheath edge is Maxwellian. By sampling along the high energy tail of this distribution, the temperature of the electrons is measurable without distorting the distribution.

The system of two equations is a fairly good model for electron temperature and charged particle number density measurements to within 20% if the following inequality holds true

$$h < a < \lambda < r_i \quad (3)$$

For the RPI Hollow Cathode Discharge (see Appendix A)

$$h \sim 10^{-7} \text{ m}$$

$$a \sim 10^{-4} \text{ m}$$

$$\lambda \sim 10^{-3} \text{ m}$$

$$r_i \sim 10^{-2} \text{ m}$$

A number for electron temperature can be obtained from the plot in Figure 2a by finding the slope of

$$\ln I_e \text{ vs } V_p$$

This temperature when used in Equation 1 will yield the charged particle

number density. The temperature is fairly accurate but the density measurement may be correct only to the order of magnitude. Equations 1 and 2 represent the inverse theory that is used for electron temperature and charged particle density measurements.

C. System Description for Langmuir Probe

The apparatus needed for taking Langmuir probe data are listed:

1. Langmuir probe (Figure 3)
2. Bellows assembly probe mount (Figure 4)
3. Monitoring Module (Figure 5)
4. HP XY recorder No. 2DR-2M
5. PAR⁺ programmable supply

The Langmuir probe is mounted in the bellows assembly and stationed at some radial position in the plasma. The probe is connected to the system as shown in Figure 1 and Figure 5. The probe voltage is set to put the probe deep into ion saturation usually taken to be -40 volts. This voltage is also the horizontal drive of the XY recorder. The current through the 100 ohm resistor in the monitoring module is the vertical drive for the XY recorder. The probe voltage is then slowly moved toward positive bias. As the probe bias is moved into positive bias, the electron current begins to rise quite rapidly, and there is a danger of burning up the probe. Usually, the probe voltage is not taken higher than +10 volts. Once the curve has been recorded, the probe is moved to another radial position and the same

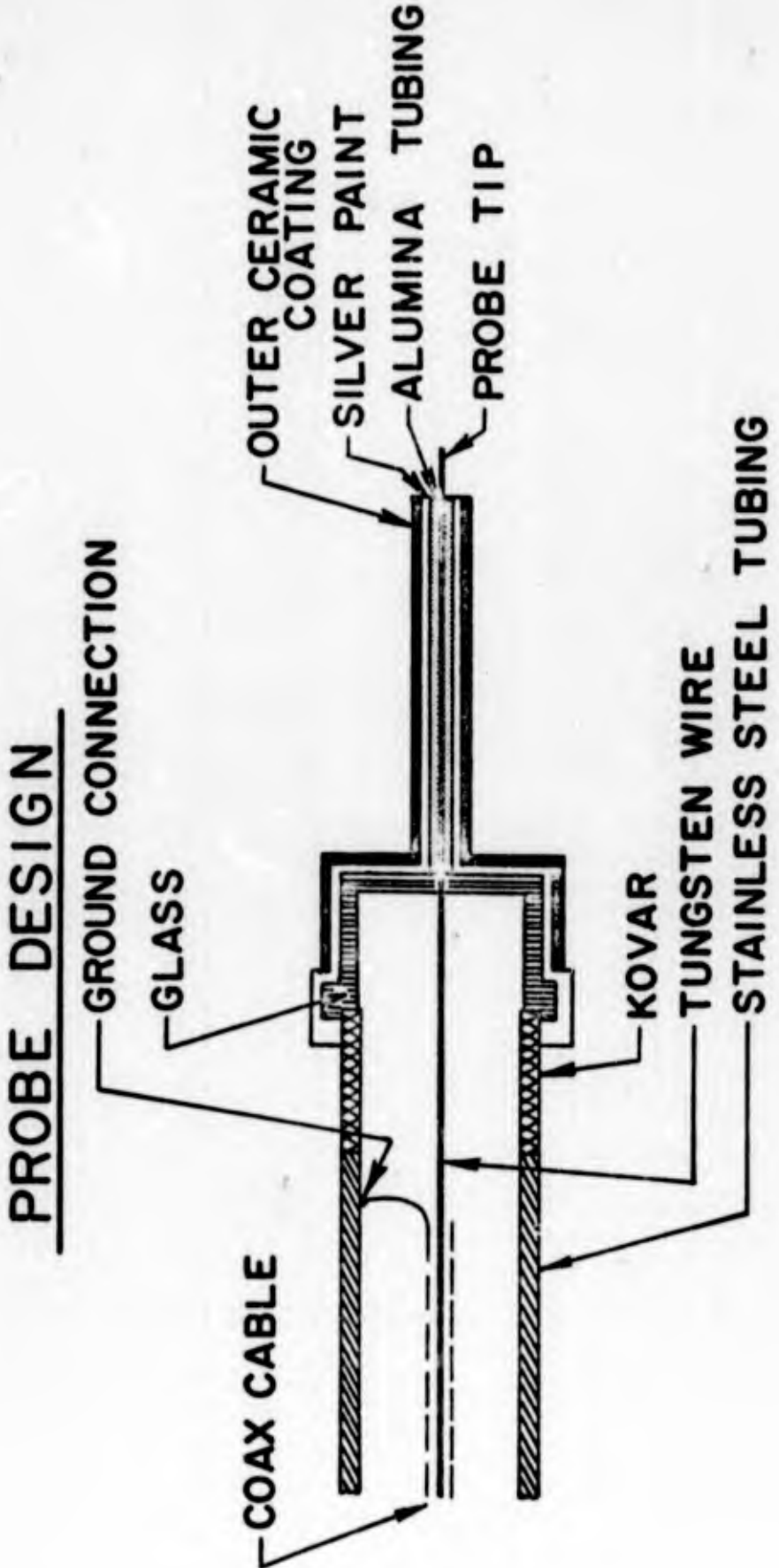


Figure 3 Langmuir Probe

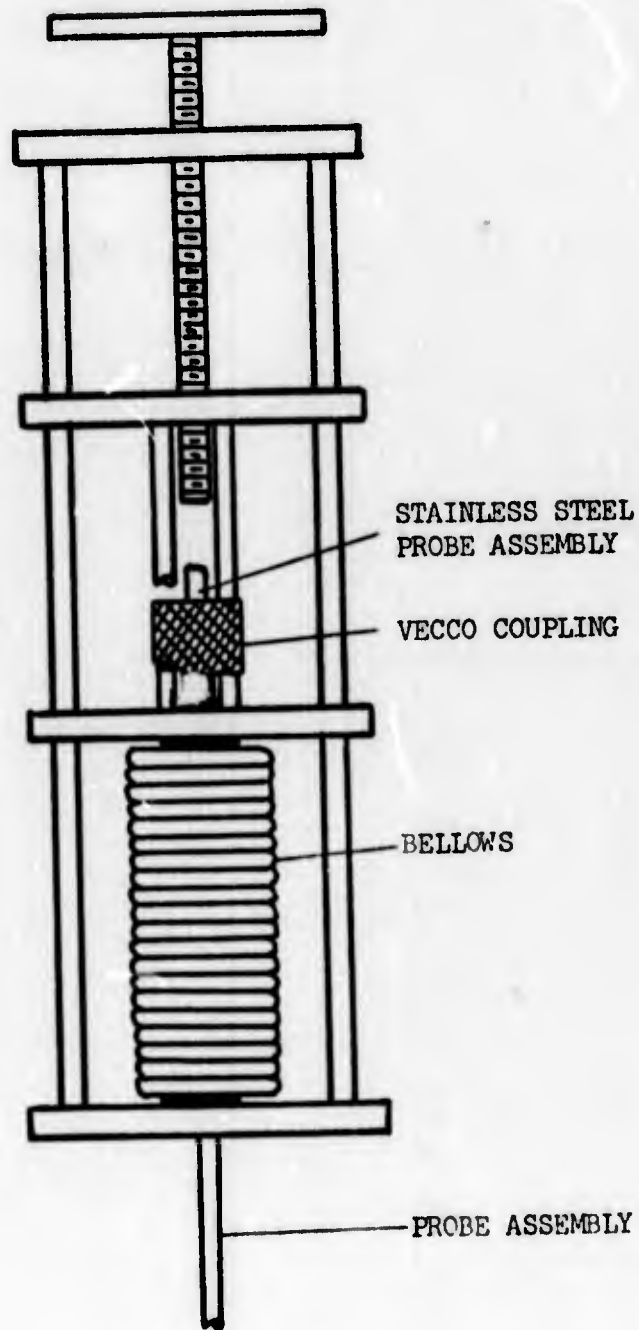


Figure 4 Bellows Assembly

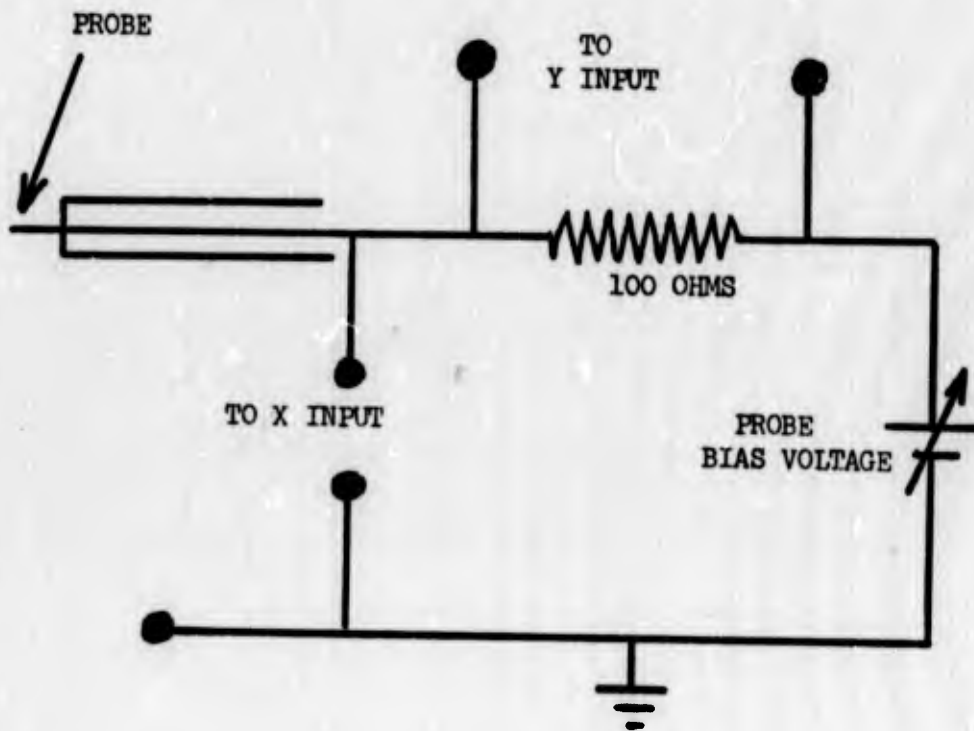


Figure 5 Monitoring Module

procedure is repeated. The procedure then followed is data analysis and will be covered in the Results Section. It should be noted that the probe tip should be oriented parallel to the confining magnetic field lines. In addition to keeping the probe away from high, damaging electron current, it is necessary to keep the probe away from the plasma core. Particle bombardment in this hot dense region will also heat up the probe and destroy it. It has been found that a too closely placed probe will greatly perturb the arc discharge and will turn the discharge off completely.

III. ION BEAM PROBING

A. Principles

1. Physics

The physics governing Ion Beam Probing are based on the Lorentz force law--a charged particle moving across magnetic field lines experiences a force that tends to make the particle curl about the field lines.

$$F = q/m (\bar{v} \times \bar{B}) \quad (4)$$

The force is proportional to the charge-to-mass ratio, q/m , the particle speed, v , and the magnetic field, B . A measure of the force and curling is given by the radius of curvature, R_c , of the particle path.

$$R_c = \frac{m}{q} \frac{v}{B} = \frac{(2mE)^{1/2}}{qB} \quad (5)$$

A change in q/m , v , or B will change the particle path. If two particles with different charge-to-mass ratios begin moving through a magnetic field from the same place at the same time, they will separate and follow different paths. The velocity changes but the speed and energy remain constant.

The IBP uses a focused beam of singly ionized ions R^+ rather than a single charged particle. See Figure 6. The beam of R^+ ions is directed towards a magnetically confined plasma perpendicular to the magnetic confining field which is oriented into the plane of the page of Figure 6; this beam follows the same curved path as the single particle. Upon intercepting the plasma, a finite number of the R^+ ions

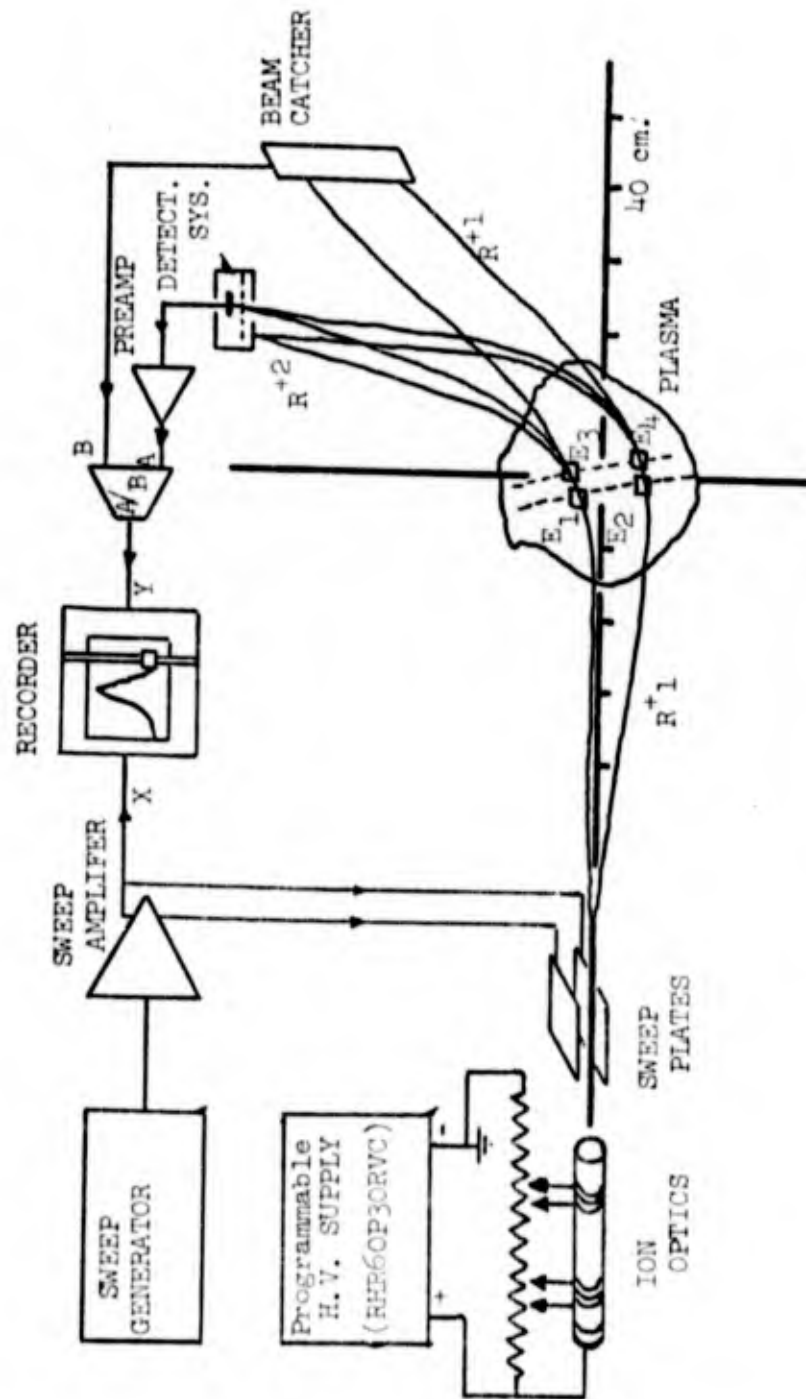
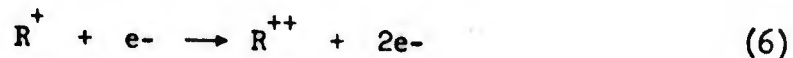


Figure 6 Beam Probing System

undergo an ionizing collision with hot plasma electrons and become doubly ionized



This reaction involves negligible momentum transfer for the ion. This can be seen from the expression for the momentum transfer from particle 1 to particle 2:

$$P_{1-2} \propto \frac{\text{Mass 1}}{\text{Mass 1} + \text{Mass 2}} \quad (7)$$

The mass of an electron ($m_e = \text{mass 1}$) is at least three orders of magnitude smaller than any ion's mass ($m_i = \text{mass 2}$); therefore, such momentum transfer is negligible. It could be argued that the speed of the particles should enter in; however, it can be shown that to have any effect at all, the electrons must have a speed on the order of the speed of light or greater. Within the collision volumes, the velocities of both R^+ and R^{++} are the same. Thus, the R^{++} ions leave the collision volume at the same kinetic energy with which they entered.

Upon leaving the collision volume, the ion experiences twice the magnetic force (Equation 4) due to the change in its charge-to-mass ratio and thus has 1/2 the radius of curvature of the singly charged ions. The particle paths separate, producing two beams; one, the incident R^+ and the other, the R^{++} beam that carries information about the plasma volume when the collision occurred.

It is important to note that upon colliding with a hot plasma electron, the ion's final trajectory is known. An appropriately placed detector will sample particles coming only from this particular plasma volume. If the R^+ beam is electrostatically swept across the plasma, the plasma volume sampled by the detector will trace a line through the plasma. This line is called a detector line. The entire plasma may be probed by using multiple detectors or by incrementing the primary beam energy in small steps. In effect, a grid of the plasma can be made in this manner. Figure 7 shows such a grid for the Rensselaer HCD. The nearly vertical lines are the detector lines; the nearly horizontal lines are the incident R^+ or primary beam paths.

2. Application

As can be seen, there are several factors that must be considered when designing the IBP system. First and foremost is a knowledge of the beam paths. This is tantamount to an explicit spatial knowledge of the magnetic field in the plasma region and the constraints assigned by the plasma machine (see Appendix A). With these constraints in mind, the optimum system configuration (i.e. type of ions, beam paths, R^+ beam source location, and R^{++} detector locations) was chosen by use of a computer program.¹³

In essence, the same beam orbits and detector locations are required regardless of ion or magnetic field. This in turn puts a definite requirement on the incident beam energy. Equation 5 can

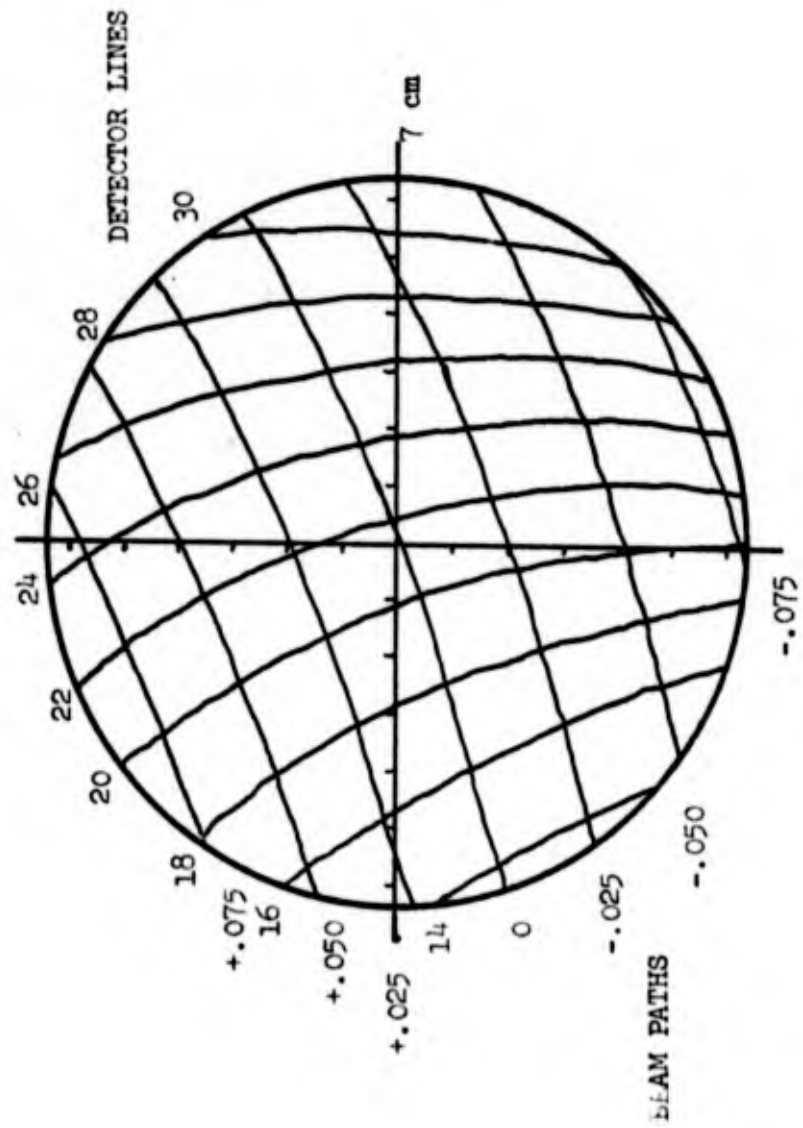


Figure 7 Detection Grid

be cast into a different form that shows the relationship.

$$R_c = \frac{m}{q} \frac{v}{B} = \frac{(2mE)^{1/2}}{qB} = \left(\frac{2}{q}\right) \left(E \frac{M}{B^2}\right)^{1/2} \quad (8)$$

The ratio of B^2/m and the R^+ beam energy are the variables whose product must be a constant for identical beam paths regardless of system configuration. It should be noted that the resulting grid mapping is not unique so an additional constraint is placed upon the system to have the detector lines and incident R^+ beam paths as close to orthogonal as possible. (Figure 7)

In addition to system configuration, there must be a knowledge of the ionizing reaction (Equation 6); it was said earlier that a finite number of R^+ ions would be ionized. This finiteness is related to a probability for the reaction to occur, the collision cross section. This knowledge places two constraints on the ion selection. The collision cross section cannot be too large so that the number of R^{++} ions created approach the number of R^{++} in the incident beam. This would lead to cumbersome data analysis. On the other hand, the collision cross section cannot be too low or else the resulting R^{++} ion signal will be masked by system noise. For this study, information about the cross sections is taken from published data.¹⁴ Ions under consideration as a result of this study are Li^+ , Na^+ , K^+ , Rb^+ , Cs^+ , Tl^+ . Table 1 shows ions currently in use and their required energies as calculated by computer program.¹⁵

Table 1

Li	42 Kev
Na	12.7 Kev
K	7.9 Kev
Rb	4.0 Kev
Cs	2.2 Kev

Ion energy for magnetic field $B = 2$ kilogauss.

3. Measurements

There are four parameters that can be made by the IBP; $n(\bar{x}_1 t)_1$, $T(\bar{x}_1 t)$, $\phi(\bar{x}_1 t)$, and $J_z(\bar{x}_1 t)$. The most primitive of these measurements is the measurement of the current that is collected at the detector (Figure 8). In general, the current collected is some function of electron temperature, $f(T_e)$ which is related to the collision cross section, T , and directly proportional to charged particle number density.

$$I \propto nf(T_e) \quad (9)$$

If the temperature dependence does not exist or temperature is constant across the plasma, the R^{++} or secondary current is directly related to the charged particle number density as seen in Figure 8. If the temperature dependence does exist, the temperature dependence must first be unwound via the collision cross section as seen in Figure 8a.

The next type of measurement is an energy measurement. By subtracting the energy the ion needed to cross the magnetic field

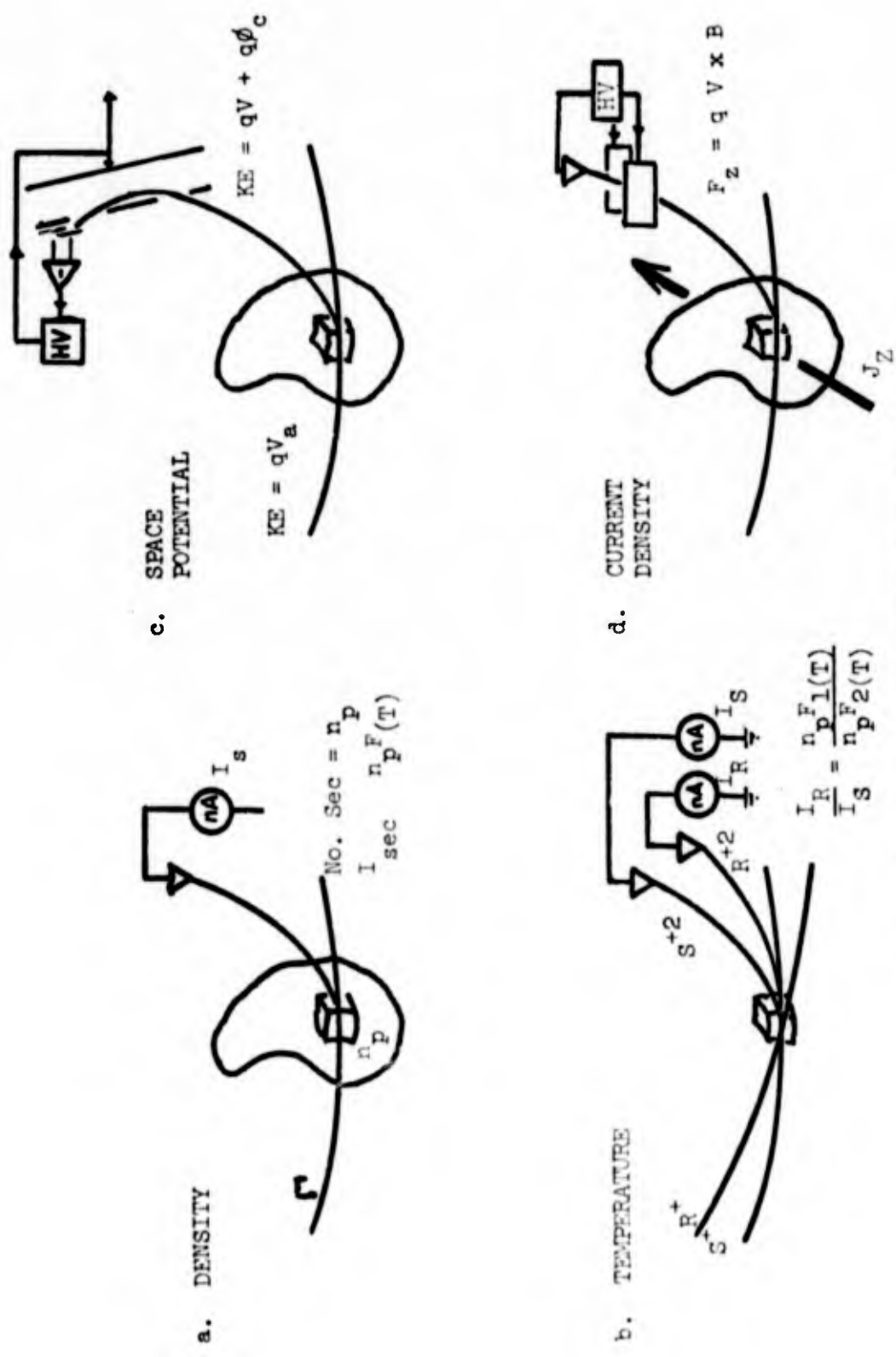


Figure 8 Beam Probe Measurements

(see IBP system description) from the ion energy at the detector, one obtains the energy gained in the plasma or the space potential ϕ .

The last measurement of current density is again based on the Lorentz force law. The plasma is a current and creates a magnetic field that winds around it. The small perturbation to the magnetic confining field distorts the ion paths by causing a small displacement out of the plane represented in Figure 6. The displacement can be related to the current distribution along the magnetic confining field.

B. IBP Theory of Density and Temperature Measurement

The theory of IBP in contrast to Langmuir probe theory is simple and complete. The secondary (R^{++}) ion current, I_s , at the detector is proportional to $I_p n_e f(T_e)$, where I_p is the primary beam current, n_e and T_e are the plasma electron density and temperature at the point of creation of the secondary ion, and $f(T_e)$ is a function representing the effective cross section for the ionizing reaction.¹⁶ By probing with two different ions, with energies scaled to produce the same beam paths, the density dependence can be eliminated as seen in Equation 10.

$$\frac{(I_s/I_p)_1}{(I_s/I_p)_2} = \frac{n_{e1} f_1(T_e)}{n_{e2} f_2(T_e)} = \frac{f_1(T_e)}{f_2(T_e)} \quad (10)$$

An expression for $f(T_e)$ can be derived from a differential reaction rate equation (Equation 11).

$$d^6R = d^3n_i(\bar{v}_i) d^3n_e(\bar{v}_e) \sigma(|\bar{v}_e - \bar{v}_i|) (|\bar{v}_e - \bar{v}_i|) \quad (11)$$

where $d^3n_i(\bar{v}_i)$ is the number of ions with velocities between \bar{v}_i and $\bar{v}_i + d\bar{v}_i$ per unit volume, $d^3n_e(\bar{v}_e)$ is the number of electrons with velocities between \bar{v}_e and $\bar{v}_e + d\bar{v}_e$, σ is the published cross section for the ionizing reactions, and $v = v_e - v_i$ is the relative speed between beam ions and plasma electrons. The distribution of ion speeds is assumed to be constant at the ion velocity obtained from the ion gun accelerating voltage. The distribution of electron speeds is obtained from an assumed Maxwellian at temperature T_e .

Consequently Equation 11 can be written:

$$R = \iint n_e \left(\frac{m_e}{2\pi kT_e} \right)^{3/2} \left\{ \exp - m_e v^2 / 2kT_e \right\} n_i \delta(v_i) \sigma(|\bar{v}_e - \bar{v}_i|) \\ \left| \bar{v}_e - \bar{v}_i \right| d^3v_e d^3v_i = n_i m_e \langle \sigma v_e \rangle \quad (12)$$

The dimensions of R are

$$[R] = \frac{\text{particles}}{\text{sec volume}} \quad (13)$$

From this dimensional analysis, an expression in terms of I_s/I_p , number density, cross section and resolution element can be found

$$R = \frac{I_s}{2q \text{ vol}_{\text{res}}} = n_e n_i \langle \sigma v_e \rangle = \frac{I_p n_e}{q v_{\text{beam}} \Lambda_{\text{res}}} \langle \sigma v_e \rangle \quad (14)$$

therefore

$$\frac{I_s}{I_p} = 2 n_e L_{res} \frac{\langle \sigma v_e \rangle}{v_{beam}} \quad (15)$$

Where L_{res} is the length of the sample volume along the primary beam path and v_{beam} is the R^+ ion velocity. Each probing ion will give a different I_s/I_p and a different $\langle \sigma v_e \rangle / v_{beam}$ or $f(T_e)$. The algorithm of Equation 10, the necessary cross section data, and the I_s/I_p data are brought together in a computer program.¹⁸ From this, the electron temperature is found. With the temperature, the density can be found by going to either ion cross section and using Equation 15.

If the reaction is no longer sensitive to temperature, then the secondary current profile are directly related to the charged particle number density. Temperature can not be found by this method. A reaction must then be found that is sensitive to temperature if temperature is to be found. The ratio of $f(T_e)_1 / f(T_e)_2$ Potassium and Sodium is found on Figure 9. Clearly, this shows a sensitivity to temperature up to 100 eV or 1 million degrees Kelvin.

C. System Description of the IBP

The complete IBP system as illustrated in Figure 6 can be broken down into three major divisions: the energetic focused ion source, the plasma, and the detector. Each division is a complex subsystem and will be discussed separately.

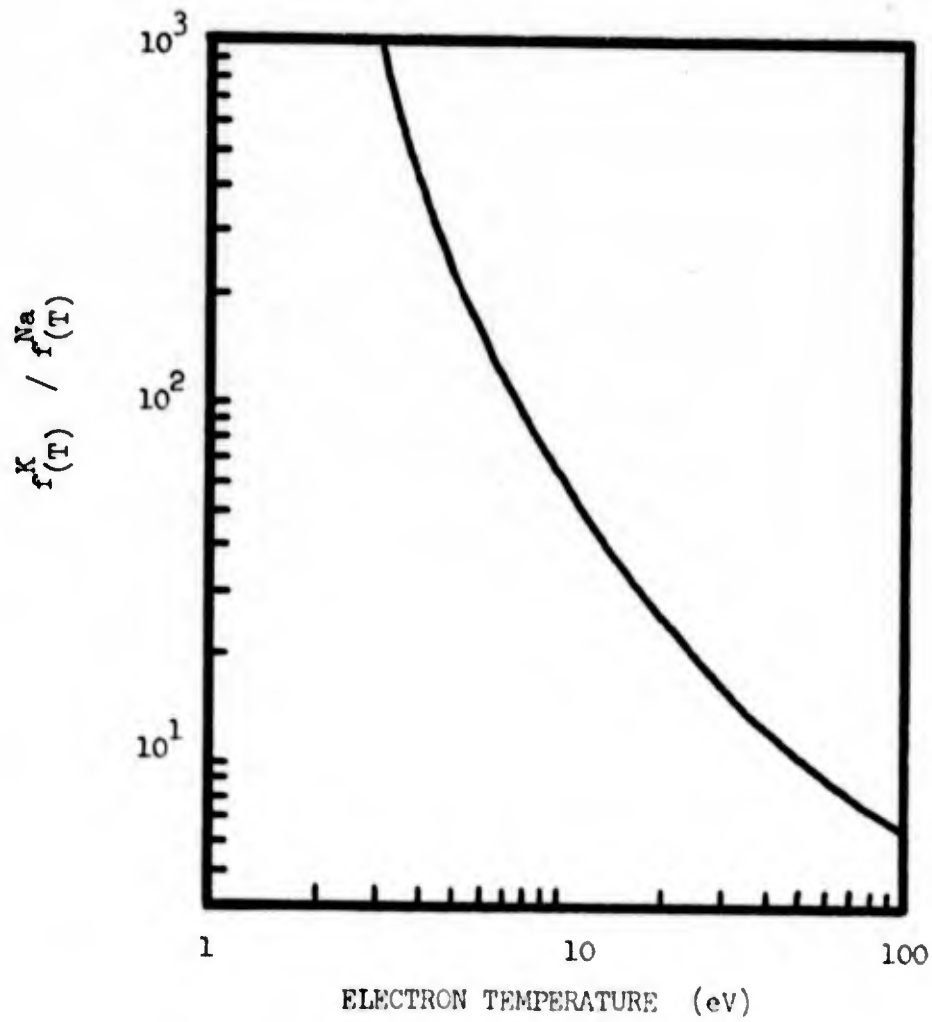


Figure 9 Plot of $r(T_e)_1 / r(T_e)_2$
for Potassium and Sodium

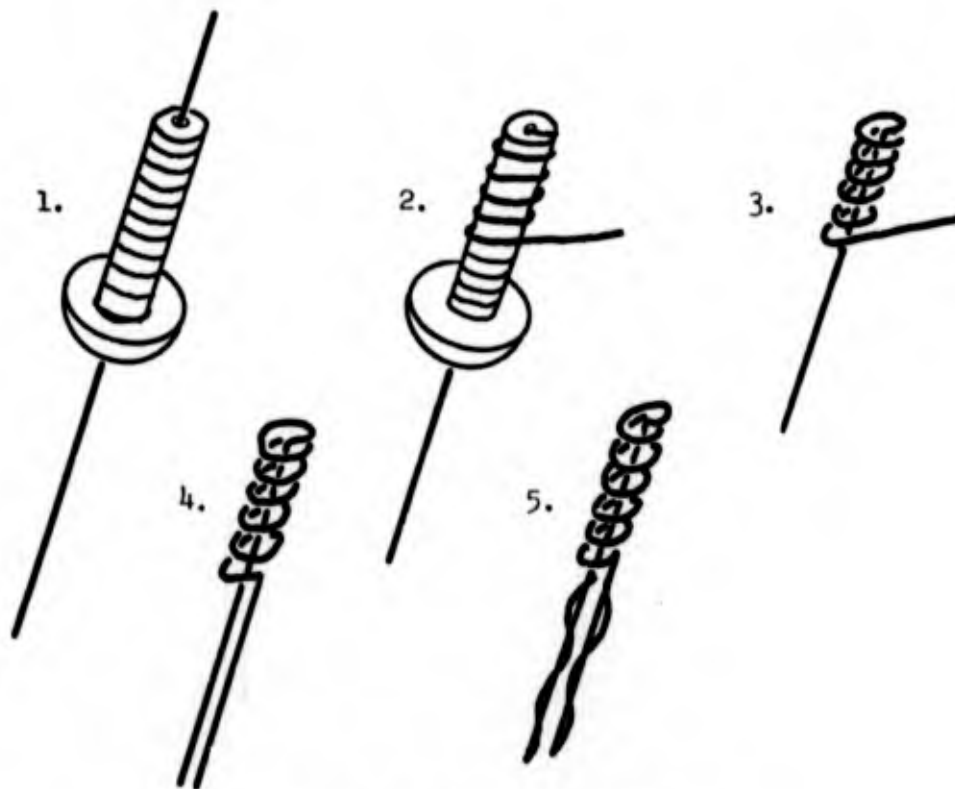
1. Ion Source

The ion source subsystem consists of three major categories: the ion gun, the electronics, and the environmental protection apparatus.

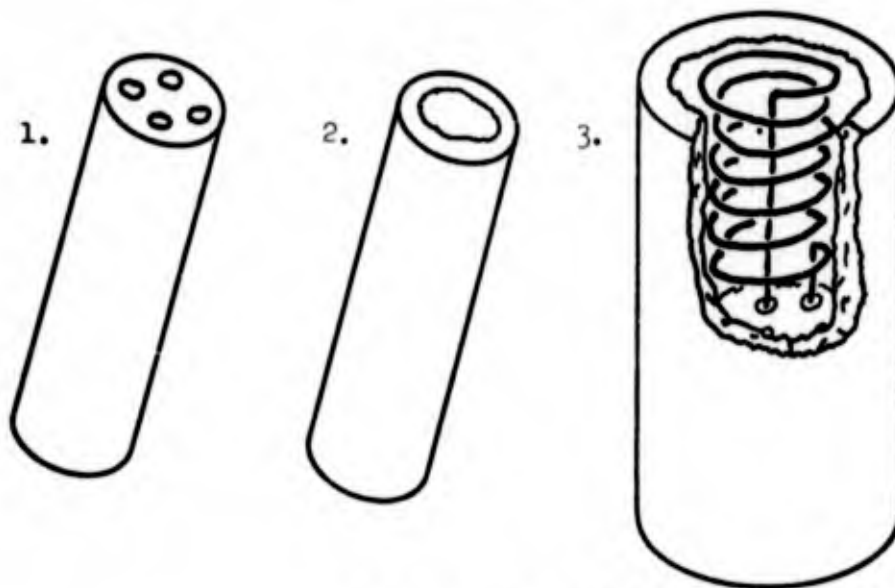
a. Ion gun. The ion gun consists of an ion supply, ion optics, appropriate deflection plates and the physical supports which connect with the rest of the IBP system.

i. Ion supply. The ion supply is derived from a thermionic emitter mounted in an accelerator analogous to the electron gun of a cathode ray tube. The ion emitter is a zeolite, a chemical that is commonly used in water softeners and petroleum cracking towers. The structure of a zeolite consists of a complex matrix with specific ions located in substitutional sites. When the zeolite is heated above a specific temperature, ions become free and are emitted from the surface. The zeolite can be obtained in a white powdered form called Mordenite. This name describes its crystalline structure. It is believed that this crystalline structure is destroyed when the zeolite is heated but this is no consequence as long as ions are emitted. The heating of the zeolite is done by packing the zeolite with the desired ion about a small heating coil made of thoriated tungsten wire, usually 10 mil. The coil is formed by wrapping the wire around a No. 2-56 screw. The screw has a hole down the middle of it to allow one half of the wire through. The wire at the top is bent over, and five or six turns are wrapped around the screw with the wire fitting the threads. Once the coil has been wrapped, the coil is then carefully turned about the screw in a direction

that will remove it from the screw. The coil must then be inspected for shorts or malformed turns. Both leads are bent parallel to the coil axis and doubled over and twisted so that the resistance of the coil is higher than the load resistance. This was found necessary because the leads would heat up instead of the coil. It has sometimes been found necessary to wrap an additional copper wire around the leads to reduce the resistance even more. See Figure 10a. An alumina rod is used for supporting the coil, insulating the wires, and serving as a container or form for the zeolite. This support is made from a commercial thermocouple insulator. The ones used here were purchased in 6" lengths with 4 holes down the length and either 3/16" or 1/4" in diameter. These came from OMEGA Engineering and had order numbers FRA364316 and FRA11614 respectively. These rods were cut into 1" lengths, and a cup was chipped out of one end to a depth that allows the coil top to be just at the surface of the rod tip. See Figure 10b. The alumina was chosen for its high melting point 2300°C. It is also extremely hard. The chipping out process is long and delicate and unsatisfactory. Several methods have been tried but none as yet have replaced chipping. Sacrificial grinding with a metal bit and an abrasive grit have been tried with a diamond studded bit. In any case, the hole must be made deep enough and wide enough so that the coil slips in without distorting. Once the coil is placed, it is best to check if any windings have been shorted. This is done visually and by placing the holder and coil in a low vacuum system 10^{-1} torr (see Figure 11). Current is passed through the coil until



a. Coil Wrapping Procedure



b. Coil Installation

Figure 10 Source Preparation

it glows. The glow should be uniform from the surface to the full length of the coil. If this is not the case, the coil has one or more turns shorted. This is easy to detect. Typical test values are from 2-8 VAC at 60 Hz with currents from 2-8 amperes. Line power controlled by a variac was used to operate the coil.

The zeolite is prepared from a commercially prepared artificial zeolite. The brand used here is Zeolon Zeolite and is obtained from the Norton Company, Akron, Ohio. This is zeolite with Sodium in the substitutional sites (called a Sodium loaded zeolite). It comes in several forms; however, a fine powder is easiest to work with.

To obtain these other loaded zeolites, there are at least two other methods. One is the Drip Method by which an amount of the Sodium zeolite is placed in a heated burette and a concentrated salt solution of the desired ion (KCl for example) is allowed to drop on the zeolite. To date, this method has not proved successful. An alternative is the Bath and Wash Method (BWM). About 20-60 ml of the Sodium zeolite is placed in a 250 ml beaker. The concentrated salt solution is poured into the beaker. The beaker is heated and the contents are agitated for about one hour; the contents are allowed to cool and settle. The liquid is removed. This is the Bath and can be repeated several times. The Wash is done by adding distilled water, agitating for about 20 minutes and allowing to settle. A portion of the clear liquid is saved and a drop of silver nitrate (AgNO_3) is added to the liquid to check for a white precipitate.

If no precipitate or very little occurs, the zeolite is loaded and washed. If not, the wash process should be repeated. For comparison, a sample of the concentrated salt solution and a sample of the clear bath liquid should be tested. When compared with the wash water, the difference should be striking. Another indication of a good wash is a rapid slowing down of the setting process by the second or third wash. The unwashed zeolite has chlorine attached to it in large numbers, thus making it big and heavy and quick to settle out. Once the chlorine is gone, some of the fine zeolite particles remains suspended and the liquid may remain milky. However, after about an hour the wash can be decanted without severe loss. A centrifuge would be helpful. It has been found that a 1 x 3 or one bath and three washes is all that is necessary for practically complete substitution of Potassium or Rubidium for Sodium. The substitution is not totally complete as traces of Na 3 orders of magnitude down from the K primary have been found in a K primary beam. Testing was done by shooting a primary beam of K^+ across the magnetic field that separates different ion species by mass.

The washed zeolite can be dried and stored or can immediately be packed in the alumina cup. It has been found that a thick water slurry of the zeolite poured or dropped into the cup is the best way to pack the cup. The assembly must be dried out and tested to see if the coil will heat uniformly. The same vacuum system shown in Figure 11 is used for this purpose although special attention is placed on monitoring the pressure inside the chamber. The pump used has a

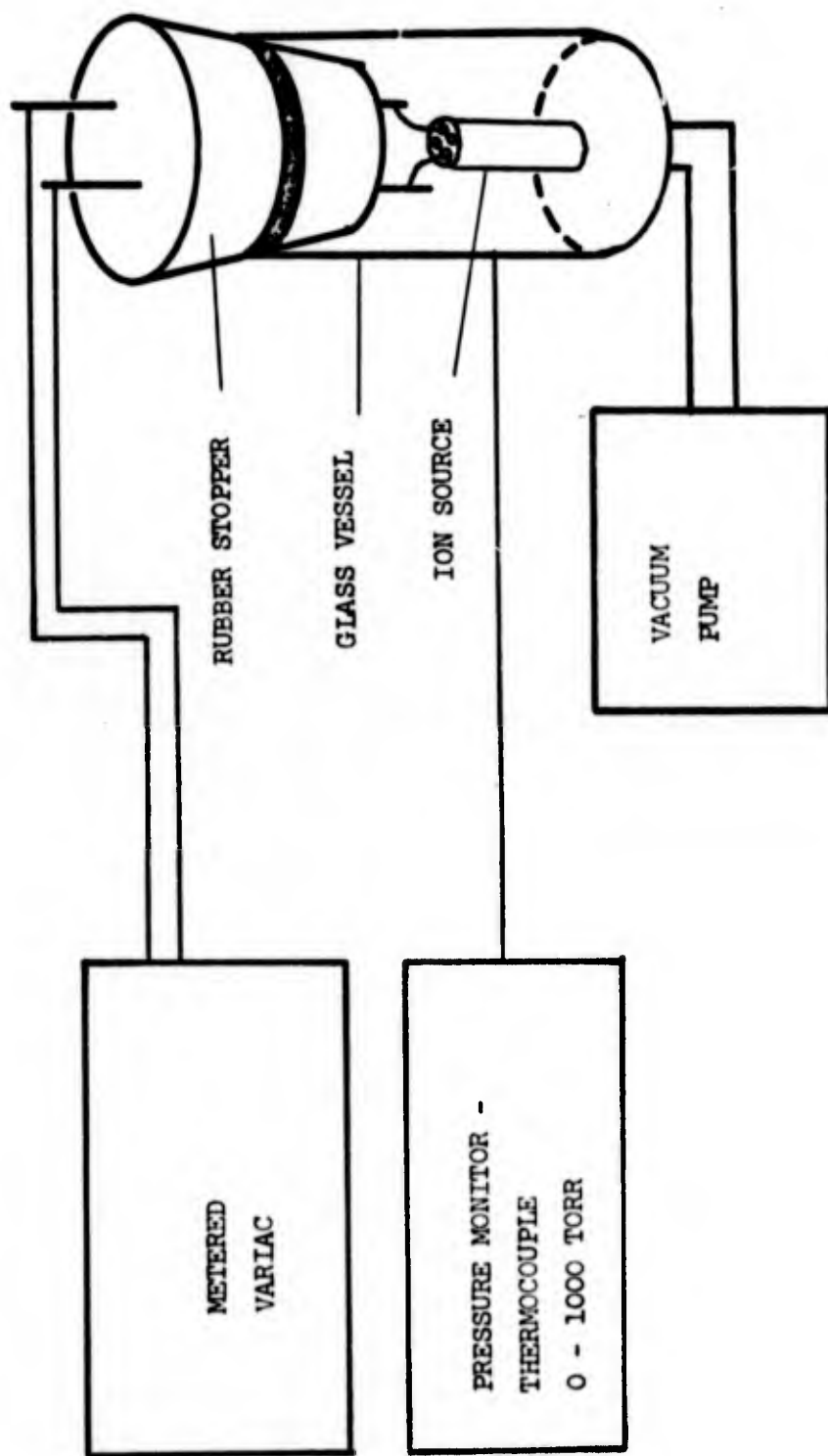


Figure 11 Ion Source Tester

base pressure of about 20 microns. With a wet source, the pump may take 10-20 hours to reach this limit. The process can be speeded up by heating the coil by the variac. The procedure is to let the pump reach 200 microns, slowly turn on the power, and never allow the pressure to rise above 250 microns. The source can be dried out and heated to hotter than cherry red within an hour. The source must again glow uniformly especially at the tip. The current voltage should be in the same range, 2-8 amperes at 2-8 VAC. When raising the power, caution is maintained so that the wire coil does not oxidize in the driven off gases, and the steam generated inside the source does not blow the source up. It was found that aging the source for about 1/2 hour at cherry red heat, allowed the source to emit well from the beginning. When the source is transferred to the IBP system or when the plasma machine is let up to atmosphere, the source picks up gas and moisture. Again caution was necessary to prevent source destruction.

Since several types of source material were anticipated (Li, Na, K, Rb, Cs, Cu) it was found necessary to develop a cataloging system with such information as source type, size, exchange process, profile pictures, focusing voltages, lifetime, etc. Figure 12 shows the form. A typical lifetime is 50 hours.

ii. Optics. The optics of the ion gun will not be heavily developed since the specifics can be found in the literature.^{19,20} Briefly, however, the gun used had an extractor structure, two three element lenses, a field free drift space and a final accelerating gap.

ION SOURCE DATA*

Source Number:

Description:

Size

Lifetime = hrs

Coil Material

Ion(s)

Construction Notes

Emission Current:

Operating Voltages

Install

Extractor

Date:

Drift Space

MA:

First Lens

Heater:

Second Lens

Remove

Date:

MA:

Heater:

*Attach Beam Profile Photos.

See Figure 13. The lenses are symmetrically operated in that the two outer elements of each lens are held at the same potential, V_1 . The center element is at V_2 . By varying the voltage ratio V_1/V_2 , a focal point from infinity down to the order of the lens size is obtained. The drift space is essential for focusing and is realized by keeping the outer elements of each lens at the same potential V_2 and maintaining a constant potential in the drift space. Enclosing the space between the two lenses with metal foil was found to be sufficient.

The final accelerating gap completes the energy boost of the ions and supplies a little focusing. The extractor is more complicated. From Pierce,²¹ the extractor structure develops collimated ion flow between the emitting electrode and the extractor electrode. In the space that follows, there is a diverging ion flow which seems to create a point source in back of the extractor electrode but not in the plane of the emitting electrode. The electrodes of this structure have a specific shape that must be adhered to for the collimated flow. The shape is determined by a solution to a mathematical expression. By using collimated flow, the efficiency of the gun is increased because more of the emitted ions are delivered to the focusing elements. This can be seen from simple optical considerations. It has been found that up to 50% of emitted current is delivered to the output pupil of the gun. Efficiency is desirable because behavior of the gun is better known and lifetime of the source is prolonged. In simple outline form, the extractor forms an imaginary point source of ions. Particles from this "source" can then be easily focused and

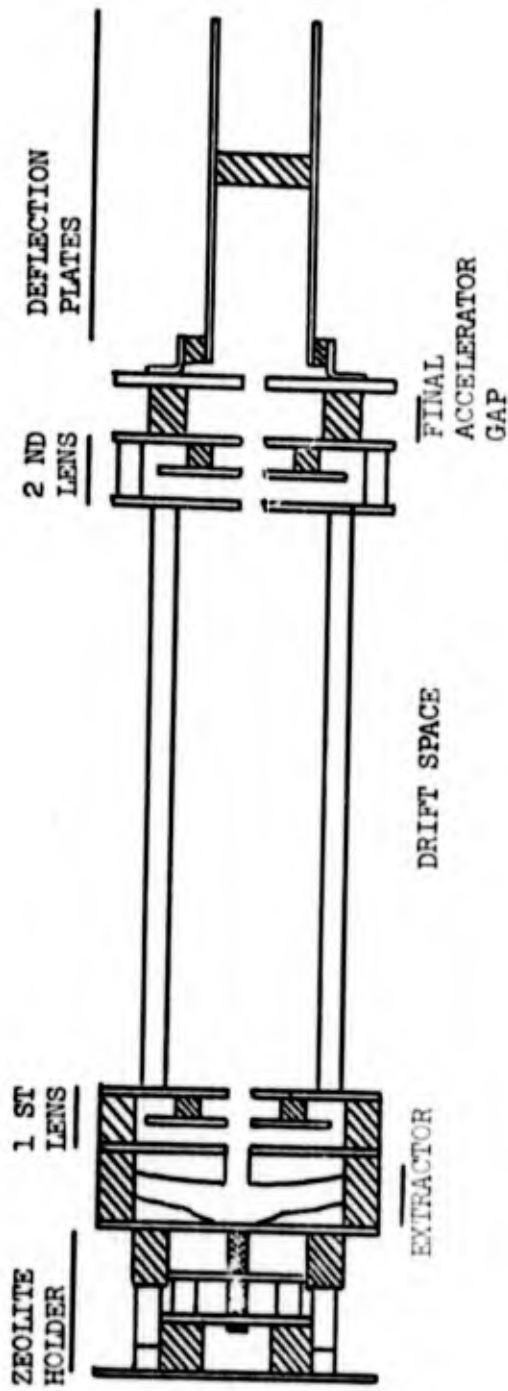


Figure 13 Ion Gun

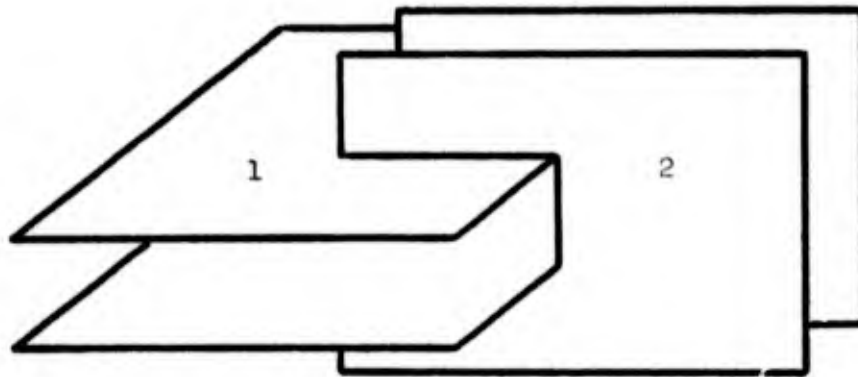
accelerated with limited loss and delivered to a specified point in the plasma as a focused beam of ions. A desirable cross section of the beam is 2-4 mm in diameter; typical values achieved are in this range.

iii. Deflection and steering. A plasma is a three dimensional object, in order to gain information about it there must be provisions for moving the probing devices about the plasma volume. The IBP utilizes in the general case two sets of deflection plates; one for steering the beam and a 90° offset for sweeping the plasma. See Figure 14a. The deflection is done by electrostatically charging the plates. Mathematically, the analysis is quite simple. The incoming beam (R^+) has an energy of $q V_{Acc}$ where V is the gun accelerating voltage. The plates have a potential difference V_p impressed upon them. The plates are separated by S_p and are L_p long. See Figure 14b. The deflection D a distance L from the plates is then

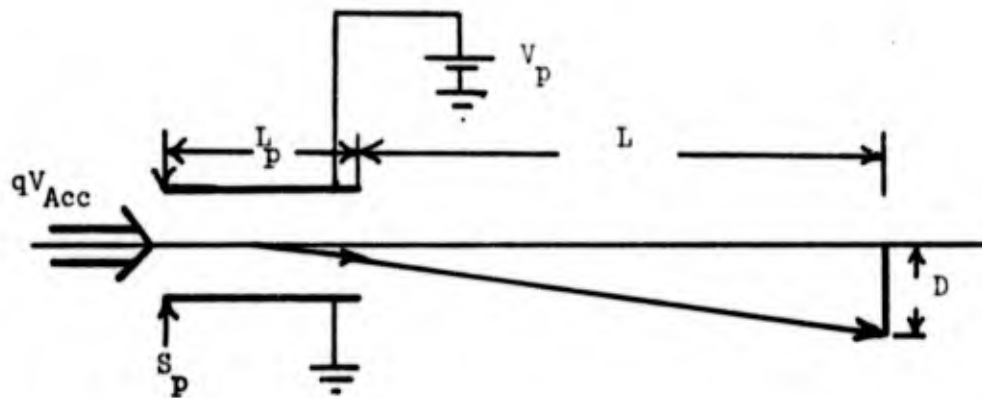
$$D = \frac{1}{4} \left(\frac{V_p}{V_{Acc}} \right) \frac{L_p}{S_p} (L_p + 2L) = \text{const.} \frac{V_p}{V_{Acc}}$$

Consequently, the deflection can be given as a percentage of the accelerating voltage. As mentioned earlier, the plasma can be mapped in a grid by electrostatically sweeping the beam across the plasma. A small volume sampled by a fixed detector is moved across the plasma along a detector line. The location of this line is determined by beam energy and detector position.

iv. Physical support. Once the ion gun was constructed there began a search for the best way to mount it to the proper port



a. SWEEP 1 and STEERING 2 PLATES



b. DEFLECTION SCHEME

Figure 14 Deflection (Sweep and Steering)

on the plasma machine (see Appendix A). Available was an opening in the stainless steel reaction chamber that was built especially for the IBP system. At first, it was thought that two problems need to be solved:

1. How to extend the vacuum envelope so it includes the ion gun.
2. How to rigidly mount the ion gun inside the envelope so that its position and beam insertion conditions were known with respect to the plasma (~ 50-70 cm away).

The method selected involved using a six inch by six inch pyrex glass (sewer pipe) cross for the vacuum envelope. By means of a 5/8" thick aluminum adapter plate and the normal six inch flanges, this cross can be readily bolted to the reaction chamber. Two of the remaining ports of the cross were used for electrical access to the ion gun since each six inch port afforded much room to spread out the high voltage terminals for the gun elements. The top and bottom ports were used for this purpose. The actual bulkhead or plate that holds the terminals is one inch thick plexiglass disk eleven inches in diameter. The terminals are spaced according to the possible electric stress, high voltage (gun elements) on one disk and low voltage (sweep, deflection, ground) on the other. The last port was kept free of any electrical wiring. Provisions have been made to use this port as an auxiliary roughing port. The system does provide a solid vacuum envelope and provides good electrical access.

The problem of gun mounting and beam insertion was complex.

It is necessary to know the position of the gun and the insertion angle of the beam; the beam orbit program is initialized on this data. For different initial conditions, there are different orbits. To solve this problem, a gun cradle was designed to fit snugly in the six inch pyrex cross and provide a rigid mount. This allows also for alignment of the gun. The gun can be aimed at the plasma and will stay aimed along that vertical plane. See Figure 15. The cradle also provides a pivot point that is necessary for the proper insertion angle. The gun remains at the pivot point by means of nylon screws that are mounted to the gun and fit into a bracket mounted on the cradle. Nylon screws were used for flexibility. Mounted to the top of the gun is a plexiglass bar that forms the rest of the lens system. At the back end of the gun the bar is drilled and tapped to accept a threaded rod. The threaded rod can be turned from outside the vacuum envelope since the rod passes through a rotatable vacuum feedthrough. Hence, the gun is rigidly mounted, aimed, and consequently, the insertion conditions are known and stable.

b. Environmental support. A plasma offers a very hostile environment to the IBP because of high background pressures, ultraviolet radiation, and cold plasma that occurs naturally in a plasma. High background pressures occur because this type of plasma is created from a gas; there must be sufficient gas around to sustain the plasma. Usually, the base pressure for the vacuum system is at least three orders of magnitude lower than plasma operating pressure. Ultraviolet radiation is a naturally occurring phenomena in plasmas. It is not

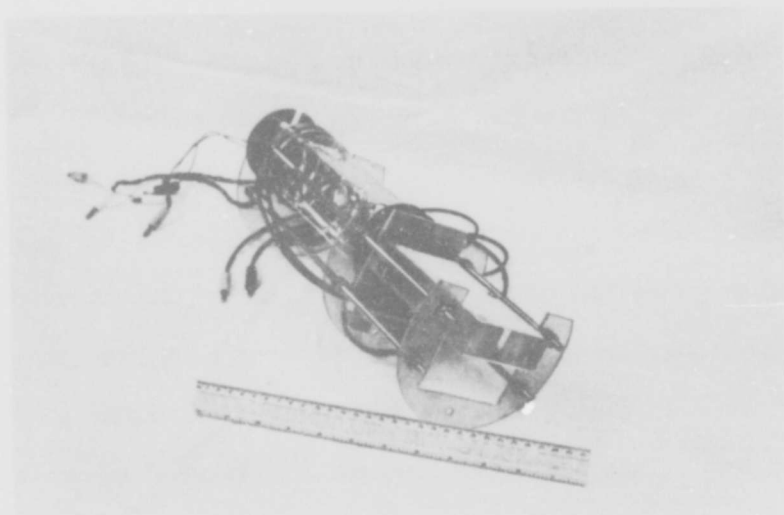


Figure 15 Support Cradle

confined by the magnetic confining field so it can irradiate the entire plasma machine volume with high energy radiation. If the radiation strikes a neutral gas atom, the gas atom will be ionized if the radiation energy is high enough. If the pressure is high enough, i.e. high background pressures, cold plasma will be created outside the magnetic confining field. This plays havoc with the accelerating electrode of the ion gun. The electrodes are loaded down; sometimes arcing occurs. This arcing played havoc with initial IBP measurements. Within the gun chamber, small sustained arcs developed, sometimes of such magnitude to shut off the gun power supply. Focusing was an intermittent phenomena at best. Clearly, the background pressure had to be lowered; the amount of ultraviolet radiation irradiating the gun volume had to be cut down; the conductance path for cold plasma created outside the gun volume to drift into the gun volume had to be lowered. These were accomplished as follows:

1. A pumping station was added just for the ion gun. This necessitated an extra piece of six inch pyrex pipe but construction was routine.
2. A differential pumping baffle was added to the gun chamber. The only openings to the gun chamber from the plasma is through the rectangular pipe 15 cm long by 1 cm wide and 6 cm tall. This pipe was made rectangular to allow the ion beam to sweep through. The baffle was made of metal to block out the ultraviolet radiation.

3. Differential pumping baffles were added to the main vacuum system. They were placed in the 6" entrance openings to the reaction chamber between anode and cathode. This isolates the chamber and allows only the plasma that is flowing from the anode to cathode to flow. In addition, these baffles lower the background pressure because the chamber is pumped by its own diffusion pump.

As a consequence of these measures, the background pressure at the anode and cathode is around 10^{-4} - 10^{-2} torr. This is desired since the plasma is created there. Inside the reaction chamber, the pressure is 10^{-5} - 10^{-4} torr. Inside the gun chamber, the pressure is 10^{-6} - 10^{-5} torr. This completely solved the gun problems. See Figure 16 and Appendix A.

c. Electronics. The electronics for running the ion source consist of five elements. The first part is the ion source heater supply. This is a 117 VAC, 15 ampere variac in tandem with a 117 VAC-10 VAC, 15 ampere filament transformer. This transformer must be capable of holding off the full gun accelerating voltage because the filaments float at this level. The requirements for the heater supply are 2-8 VAC at 2-8 amperes but floating at a high D.C. potential.

The main element of the ion gun is a Spellman High Voltage Electronics Corporation supply - RH30P60RVC, 0-60KV DC, 0-500 μ a remotely programmable. It is highly regulated and ripple free. The output voltage can be manually dialed in or it can be remotely controlled.

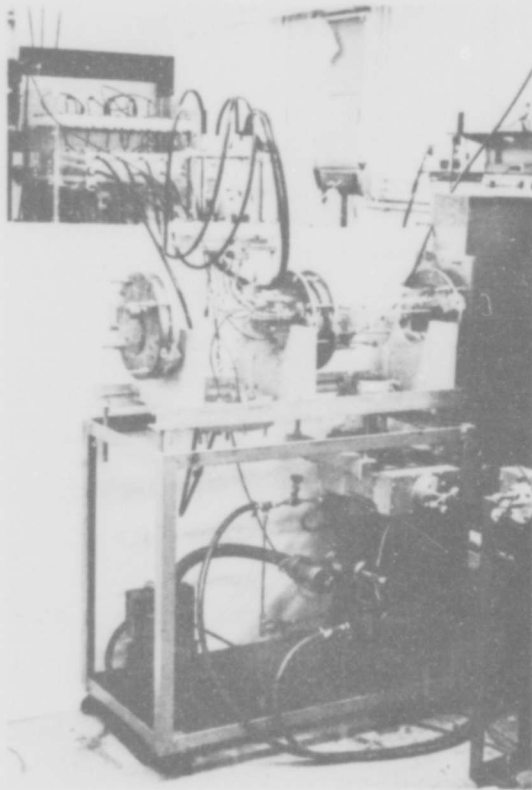


Figure 16 Ion Gun Differential Pumping System

While the Spellman supply creates the main accelerating voltage, the other gun element voltages are created via a resistor divider circuit. This circuit was chosen for its simplicity and in theory would maintain a constant ratio between all potentials as the input power supply was varied. The circuit contained a total of 200 megohms in lumps of 10 megohms. Three of the 10 meg units were made up of four 2 megohm resistors and a combination of a 1 megohm resistor and a 1 megohm potentiometer. Three variable output voltages were obtained from this supply. A fourth was added later but only as a clip lead wire. It was found that the carbon composition resistors are inadequate for high voltage work; they do not maintain their resistance value at high voltages. A better design using high voltage resistors is in the planning stage, these resistors are significantly more expensive but they do not sag under high voltage stress.

The fourth equipment subsystem is the sweep supply whose function is to electrostatically move the beam across the plasma. The output required to do this can be a ramp, a triangle, or a sinusoid with variable amplitude and D.C. offset; the circuit (Figure 17) creates two identical signals; e.g. ramps. The circuit adds a 180° phase shift to one signal. Each signal is amplified separately and applied to one of the two sweep plates. The potential across both sweep plates is the desired sweep voltage. The high voltage buss is supplied by two Spellman 0-10KVDC supplies. It should be noted that the sweep supply cannot be heavily loaded because the

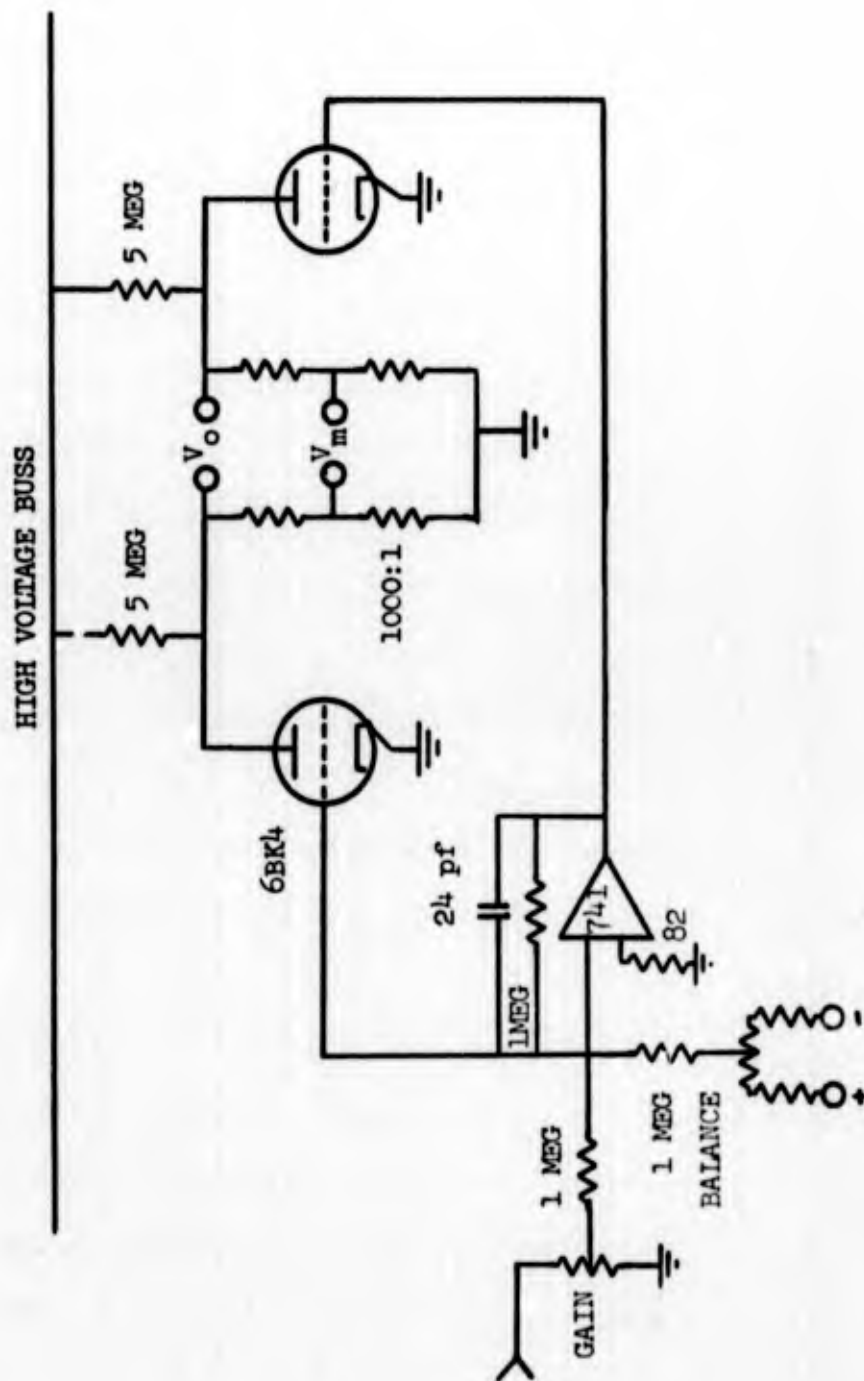


Figure 17 Sweep Amplifiers

Spellman supplies cannot handle such a load. Consequently, the time constant of the circuit is long, fast sweep rates and hard to obtain. At present, a good sweep signal is obtained at 1 KHz and a fair one at 10 KHz. A trade off between safety and speed was made to obtain a reasonable degree of safety. Recently, a new power supply from Hipotronics, Brewster, New York, replaced the 0-10KV DC Spellman. This 0-10KV supply was ordered with a current limiting safety feature. The phase shifter uses a Nobatron 0-30V DC supply.

The last element is a H.P. function generator. Not only does it supply the specific function shape for sweeping but it also supplies a synchronizing pulse to establish a time base for all electronics. A Tektronix 541 scope is used to monitor the sweep signal.

2. Detectors

a. Types. The type of detector used depends upon the particular application. In general, there are two major types of detectors, beam samplers and beam catchers. A beam sampler measures extent or spatial distributions of the beam. A beam catcher measures how much beam is present by collecting all incident beam particles; over time, this detector measures amperes of beam current.

The basic requirement of the IBP system is a focused beam of ions, a figure of merit is a beam cross section less than 5 mm at half width and an amplitude of 1 to 5 microamperes. To measure the beam, both types of detectors are required. The beam is swept across a beam sampler, generally a fine wire. From convolution theory, such a sweep tells the true extent or width of the beam if the wire is

infinitely thin. A finite sized wire establishes an upper bound to beam width. The beam width is a parameter that must be known because it is one dimension of the small plasma volume or resolution element that is probed by the IBP. The resolution element determines the lower bound on plasma fine structure. The beam current size can be monitored by a metal plate downstream from the beam sampler. In a fully developed and operational IBP it is still necessary to focus the beam or check on beam focus since sources will need to be changed periodically. A ladder of wires of known spacing has been found to be a convenient calibrated focusing tool.

Beam samplers are used to determine the resolution element of the IBP. This is done by sampling the beam along several points of beam travel, before the beam intercepts the plasma. This measurement checks on the divergence of the beam.

Beam sampling is also used when developing multiple ion source techniques. The samplers are placed downstream from the plasma outside of the gross effects of the magnetic field. From Equation 5, it can be seen that there will be a separation of R_1^+ and R_2^+ .

For the operational IBP, the sole detectors are beam catchers; one beam catcher collects R^+ primary current, the other collects R^{++} secondary current. Both currents are needed for normalization. The R^+ detector is a sheet of metal whose dimensions is the image of the plasma at the R^+ detector location. The R^{++} detector is a 2 x 2 cm sheet with an iris that passes a current whose spatial extent is the size of the plasma resolution element imaged at the detectors. The

computer orbit program shows that there is a 2X magnification; a 1 cm x 1 cm iris is imaged down to a 1/2 cm square at the plasma. The other part of the resolution element, of course, is the beam's cross sectional area in the plasma. The R^{++} detector on the RPI HCD is capable of moving along a line perpendicular to the plasma in a horizontal plane about 50 cm above the plasma. R^+ detector signals are on the order of microamperes; R^{++} detector signals are on the order of nanoamperes or less. Normalized data is given as nanoamperes R^{++} /microamperes R^+ . This is the desired data as seen from Equations 10 and 15.

b. Environmental protection. Early attempts to make IBP measurements were failures for many of the reasons cited earlier for the ion gun failures. The major difference is the following. Instead of turning the R^{++} detectors off as happened to the gun, the R^{++} detectors displayed a high noise level and a contamination by R^+ primary ions that were scattered from neutrals. The problem centered around solving two problems.

1. Plasma noise due to high background pressure, ultraviolet radiation and cold plasma.
2. Primary beam scattering.

To eliminate cold plasma noise, the detector was placed in a Faraday shield that can be grounded, floated, or placed at any specific potential that reduces noise. Grounding the cage has been found the best.

To eliminate ultraviolet radiation, two steps were taken. Baffles were hung from the detector to limit the ultraviolet radiation to only line of sight exposure. Care had to be taken to ensure that the baffles did not extend into the secondary orbits. In addition, the side of the detector that faced away from the detector was opened up to allow more efficient pumping of the detector volume. As mentioned before, the lower the background pressure, the lower the noise becomes.

To eliminate primary scattering, vertical baffles were hung along the centerline plane of the reaction chamber, parallel to the plasma. This allowed only primary ions destined for the plasma to get through. Since the plasma-bound R^+ ions follows orbits that miss the detector, the problem is solved. Indeed it was. Before the baffles were installed, there was a spurious current level of ~ 0.1 nanoamperes. In a plasma of low density and/or temperature, this was all the secondary current that could be expected. Clearly such a scattered primary R^+ current would mask the secondary R^{++} current. After the baffles were installed, the scattered primary current dropped considerably. At system base pressure 10^{-6} torr, the scattered primary current was around 10^{-3} nanoamperes. At plasma operating pressures of 10^{-3} torr, this current increased to $2-5 \times 10^{-2}$ nanoamperes. The primary baffles also brought plasma noise down. These baffles cut the pumping volume nearly in half so the pumping is more efficient in the detector area. Figure 18 shows the detector used.

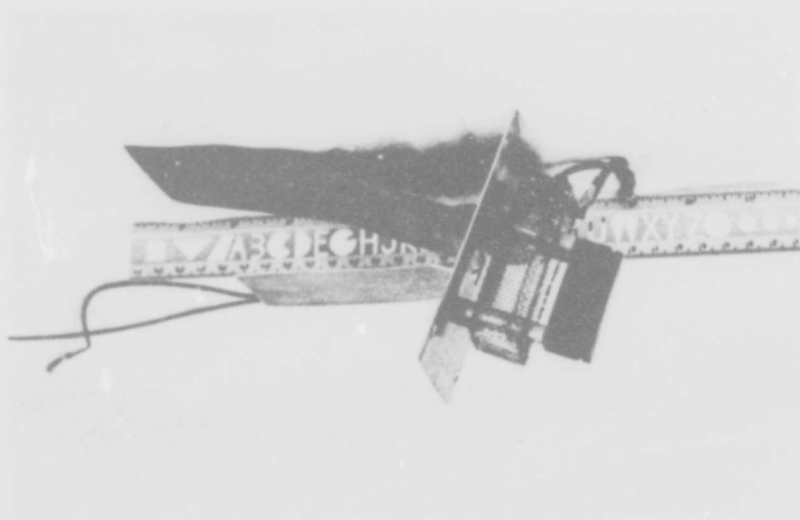
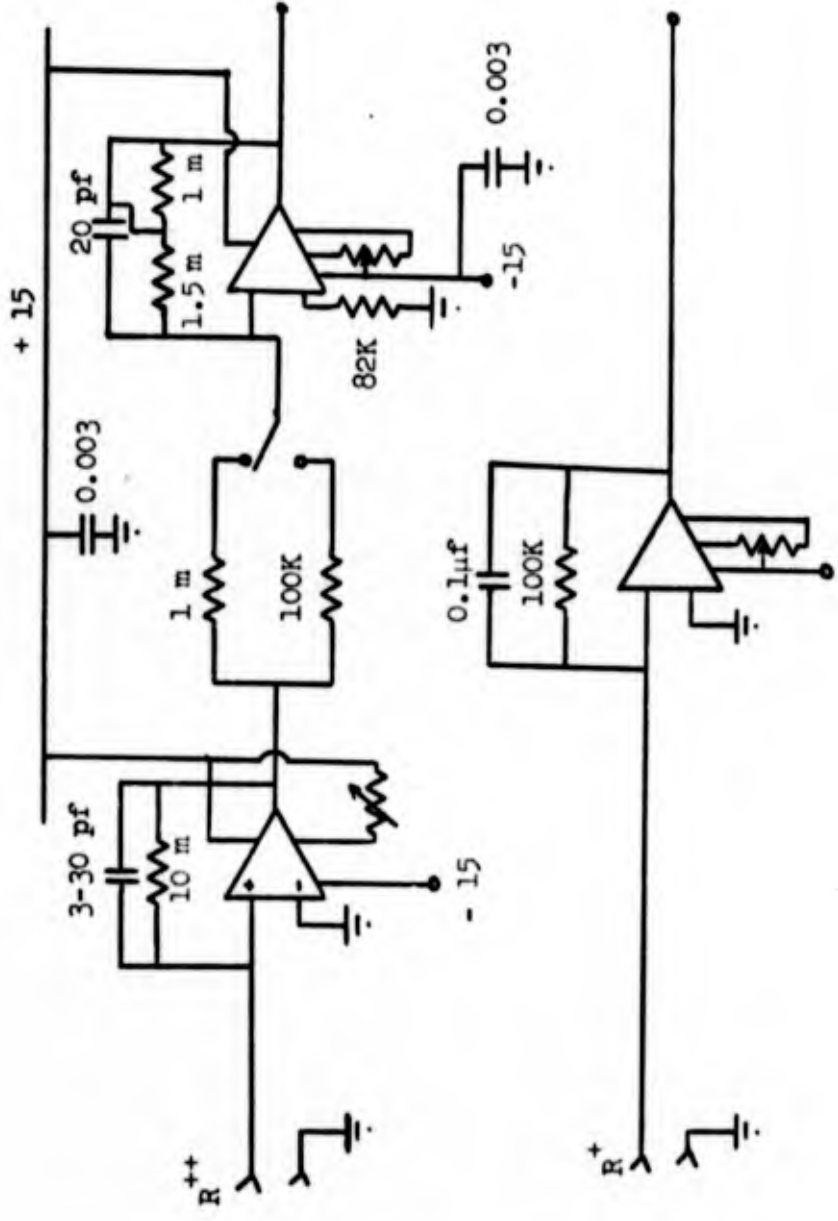


Figure 18 Detector (R^{++} ions enter from the right)

c. Electronics. There are a variety of signals that are of interest in the IBP system. When preparing the system for operation, beam profiles, location of the beam, and beam magnitude are desired information. Current levels are in the microampere range so the operational amplifier plug ins for a Tektronics type 556 oscilloscope were used. The plug ins were used in the low input impedance, current amplifier mode because this affords the secondary ions a low impedance path to ground. Charge will not accumulate. If the high input impedance voltage amplifier were used, the charge would tend to build up and would take a longer time to decay away thus distorting the beam profile. When measuring R^{++} or secondary current, more gain and quieter electronics are needed so an amplifier string of op amps with a low input impedance current amplifier as an input and a high input impedance amplifier as the output. The output had two gain levels, either 25 mv/nanoampere or 250 mv/nanoampere. This preamp is also frequency tailored for a high frequency cutoff at 1 KHz and for low frequencies, the preamp is DC coupled. This arrangement eliminates higher frequency noise and allows for slow measurement to average out the rest of the noise. See Figure 19 for the circuit diagram.

The preamp is connected to a 556 scope. When used in this configuration with no plasma, signal as low as 0.004 nanoamperes could be measured. Electronic noise is on the order of 0.005 nanoamperes. As yet, this level has not been reached because of plasma noise.



AMPLIFIERS ARE PHILBRICK 1026

Figure 19 D.C. Amplifier

When taking data, another important piece of electronics is a secondary/primary current normalizer. This can be obtained commercially or can easily be built from standard components.

For recording the data, two courses of action are followed. The simplest and least useful approach in terms of numbers is a polaroid picture of a scope trace, an oscillogram. This is generally used in the system development stage and during system check out prior to large amounts of data taking. At present, meaningful data is recorded by means of a HP XY recorder No. 2DR-2M. At a later date, this data is retraced manually, and by proper scaling, the same current/position data is measured and punched on a paper tape compatible with the G.E. Mark II time sharing computer. The analog-digital conversion is done by a Dymec Data Acquisition System (DAS).

IV. EXPERIMENTAL RESULTS

Charged particle number density and electron temperature data for a hollow anode, hollow cathode discharge in Helium have been taken with both a Langmuir probe and an Ion Beam Probe. The results of these measurements are presented in this chapter along with a brief discussion of how the data were reduced.

A. Langmuir Probe Data

Langmuir probe data was obtained by biasing the probe with respect to the anode (Figure 1) and plotting the measured current versus voltage with an XY recorder. This data was taken at several radial positions away from the arc core and resulted in a probe curve for each position. The curve is plotted with electron J_e positive. Each probe curve will yield n and T_e from Equations 1 and 2. Charged particle number density, n , can be found from Equation 1 when the ion saturation current, I_{ion} , and electron temperature, T_e , are known. T_e can be found from the slope of the $\ln I_e$ versus V_p curve as seen in Equation 2. This requires that the ion current contribution to the probe curve be subtracted off. This is done as shown in Figure 2a by establishing a straight line from ion saturation (I) into region IV that best follows the ion current contribution (line A). When this line is subtracted point by point from the probe curve the remainder is electron current.

The data reduction process can be done manually or by computer. When done manually, the process is slow and arduous, and

is done as follows:

1. Determine the electron current I_e in regions II and III of Figure 2a by
 - a. drawing the ion current line A
 - b. using dividers measure the difference between the probe curve and line A in II and III. This is the electron current at that value of probe bias V_p .
2. Calculate the natural log of I_e
3. Plot $\ln I_e$ versus V_p and fit a straight line through the points
4. Determine the slope of line, S.
5. Calculate $T_e = e/kS$
6. Calculate
$$n = \frac{(\pi M_{ion}/2kT_e)}{I_{ion} e (\text{Probe Area})}$$

At RPI there are two computer programs that reduce Langmuir probe data. The first is PROBE.²² Step 1 must be done manually. The data that is fed into the program are three points of (I_e, V_p) near the knee of the probe curve and the value of I_{ion} at maximum negative probe bias. The other program is GLOWPROB. This program was written for this thesis. Steps 1 through 6 are done by the program. All line fitting is done by a least squares fit. Copies of both programs are found in Appendix B.

Figures 20 and 21 show a plasma profile of T_e and n respectively versus radial position from the core. The data reduction was done by GLOWPROB. The plots show rising density and electron temperature as

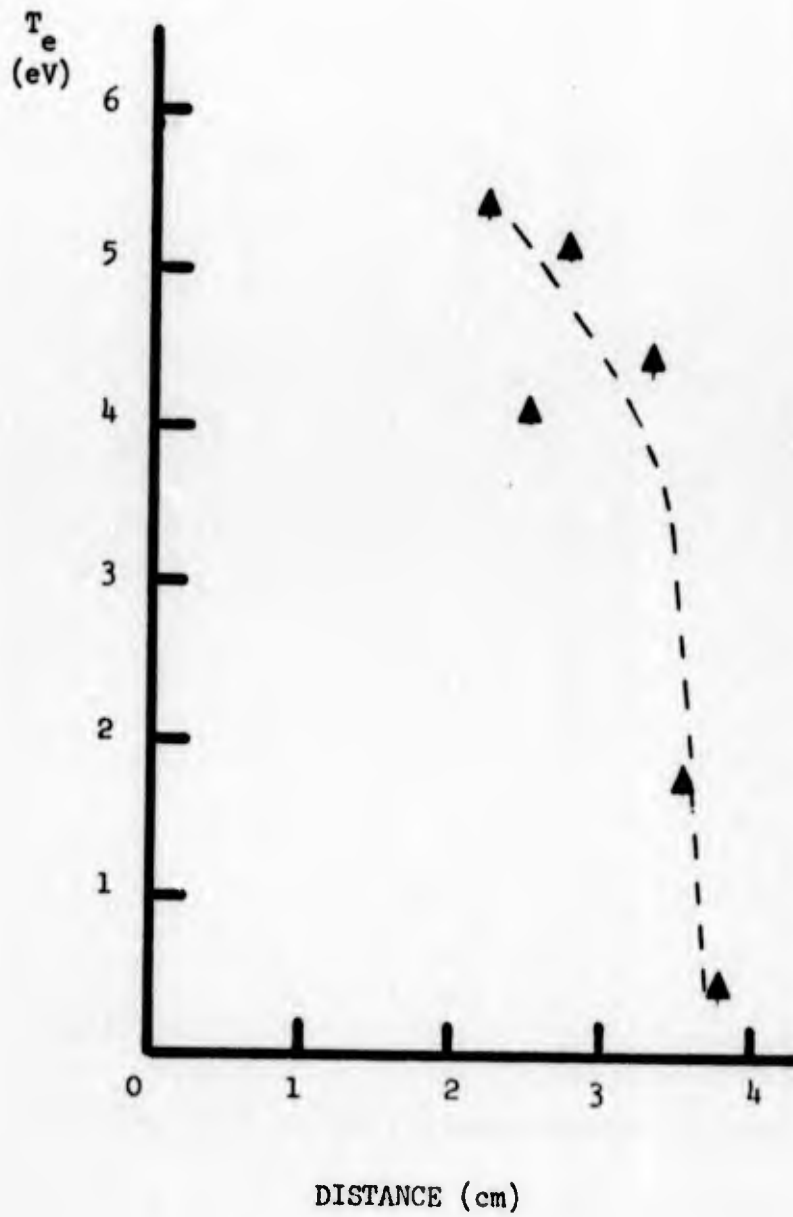


Figure 20 Langmuir Probe Electron Temperature
 T_e Versus Distance R From Arc Center
Arc is Helium



Figure 21 Langmuir Probe Number Density n Versus Distance From Arc Center. Arc is Helium

the core is approached although the temperature plot shows some scatter. The rise in both is expected; the core is denser and hotter.

B. Ion Beam Probe Data

Density and temperature measurements come from the most primitive of IBP data, the R^{++} current collected. This is proportional to $nf(T_e)$. The form of this data is a plot of the magnitude of $nf(T_e)$ versus radial position along a particular detector line. A collection of such plots along different detector lines will form an isometric projection of $nf(T_e)$ across the whole plasma cross section. This is seen on Figure 22. This is an isometric plot of $nf(T_e)$ of the Rensselaer arc taken with a Potassium ion source. This is a grid mapping of the plasma corresponding to the mapping shown in Figure 7 for the Rensselaer HCD. This figure was made by physically moving the detector to different detector line locations.

The separate profiles of n and T_e are again obtained through a computer program.²³ The raw data, the $nf(T_e)$ plot, is recorded on a sheet of paper by means of an XY recorder and is saved for later data reduction. The raw data for Sodium and Potassium beams is seen on Figure 23. The data reduction begins by an analog to digital conversion of the $nf(T_e)$ plot to a punched computer tape. This is done by retracing the plot with the XY recorder. By proper scaling, the output of the XY recorder as punched will be the radial distribution of I_s/I_p (see Equations 15 and 10). The computer program requires the collision cross section for each ion used. With this information, the program yields T_e and n versus radial position.

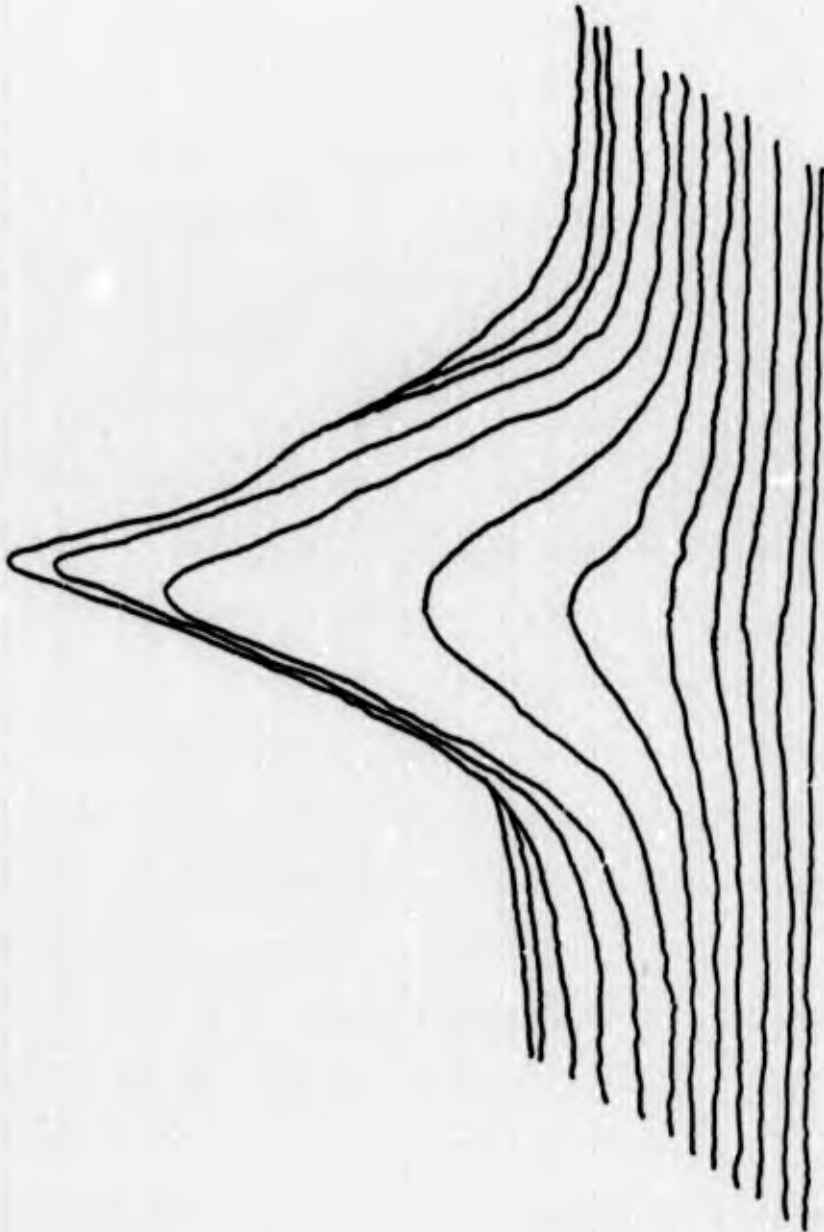


Figure 22 Isometric $nf(T_e)$ for Potassium
Ions in a Helium Arc

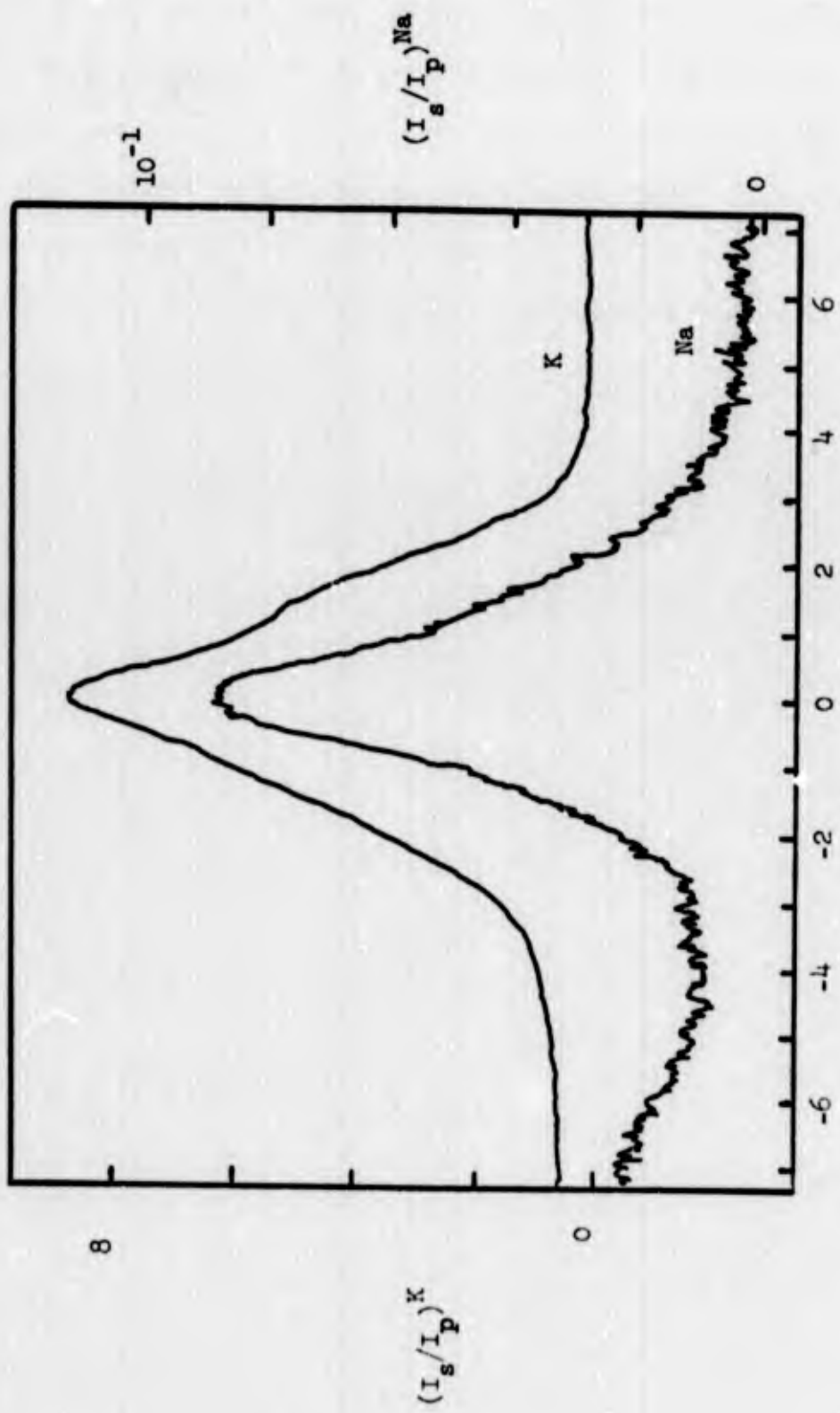


Figure 23 Raw IBP Data I_s/I_p for Potassium and Sodium in Helium

This is plotted in Figure 24. As expected, the temperature and density rise as the core is approached. However, very near the core, the density drops, this is something that has never been seen before. This is the first time the profile has been taken all the way through the plasma. The measurements do not go out too far, however. The $n_f(T_e)$ signal was buried in the noise at about 2 cm from the arc center. This is a point for further system development.

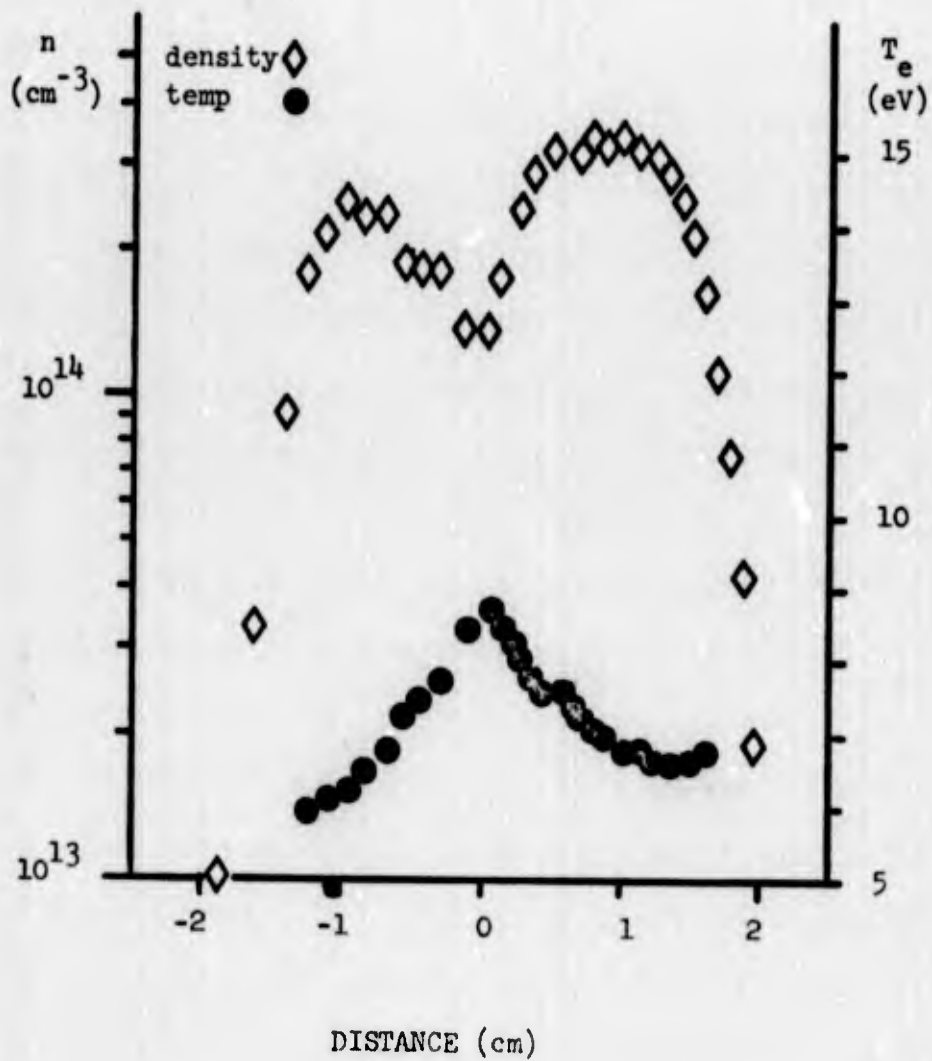


Figure 2h. Number Density n and Electron Temperature T_e for a Helium Arc

V. DISCUSSION

The original plan for the thesis was to obtain data that would compare Langmuir probe and IBP measurements. Figures 20, 21 and 24 show that there is practically no overlap. This is due to the fact that the Langmuir probe cannot be used in the core, and at present, the IBP cannot be used at large radii. The two figures are plotted together in Figures 25 and 26 for n and T_e respectively. Although there is no overlap, there appears to be a continuous curve for density as the change is made from IBP to Langmuir probe. A curve could be drawn for temperature although the fit is more arbitrary. Because there is no overlap, all that can be said is that the transition is fairly continuous between the two modes of measurement. Clearly for any comparison, there must be an overlap.

The Langmuir probe is temperature limited; the IBP is noise limited. Any one or both of the modes must be extended to make the comparison. It is thought that the Langmuir probe can be moved through the plasma if it is driven through quickly. The IBP can be made sensitive with a different detector--the Electrostatic Energy Analyzer. Much consideration is being given to both techniques at this time. Several experiments are being planned with a driven probe and the more sensitive detector.

Of the work done so far, it can be said that the IBP does have a definite advantage over the Langmuir probe in that it can measure all the way to the core of the plasma. Also, it measures both

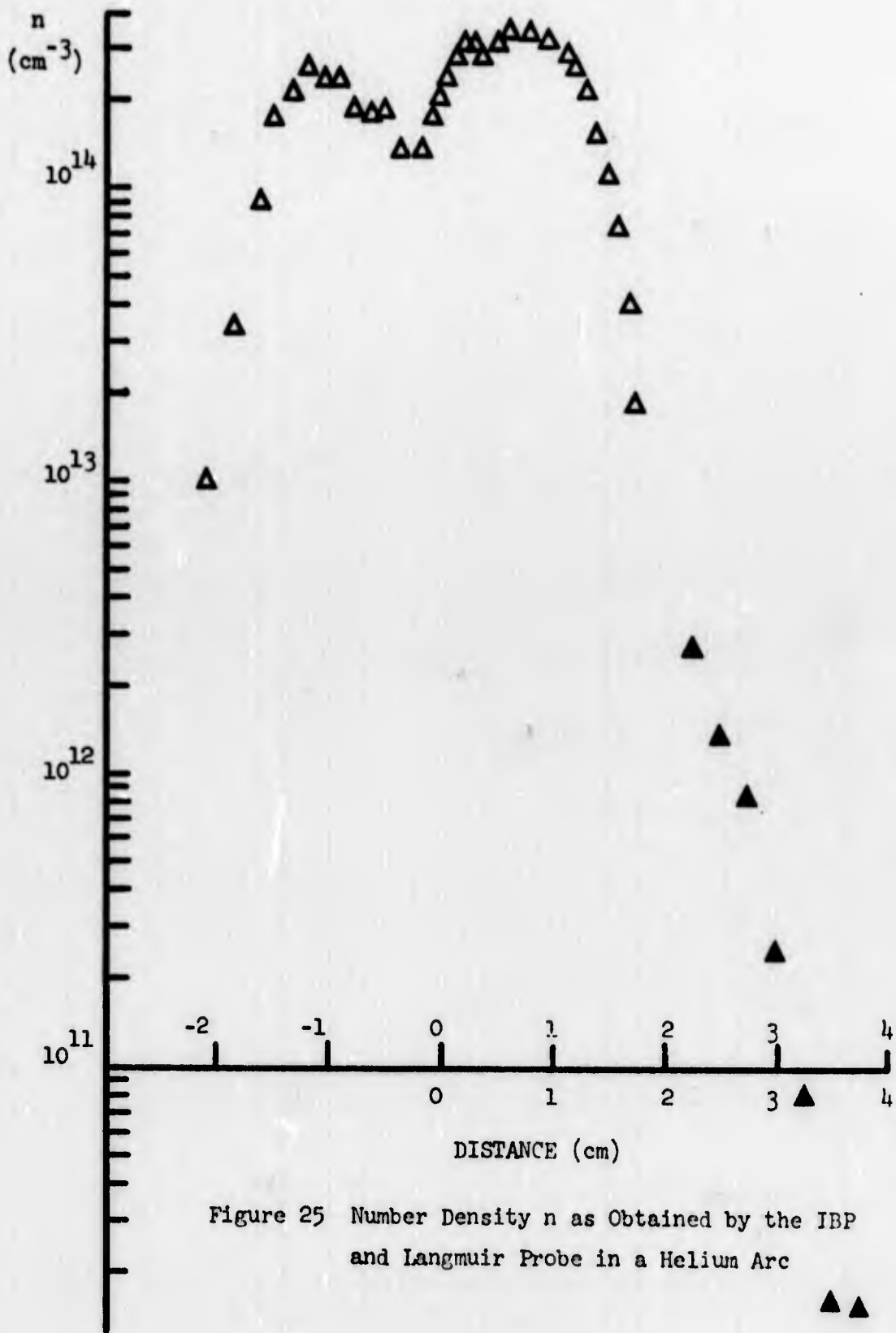


Figure 25 Number Density n as Obtained by the IBP and Langmuir Probe in a Helium Arc

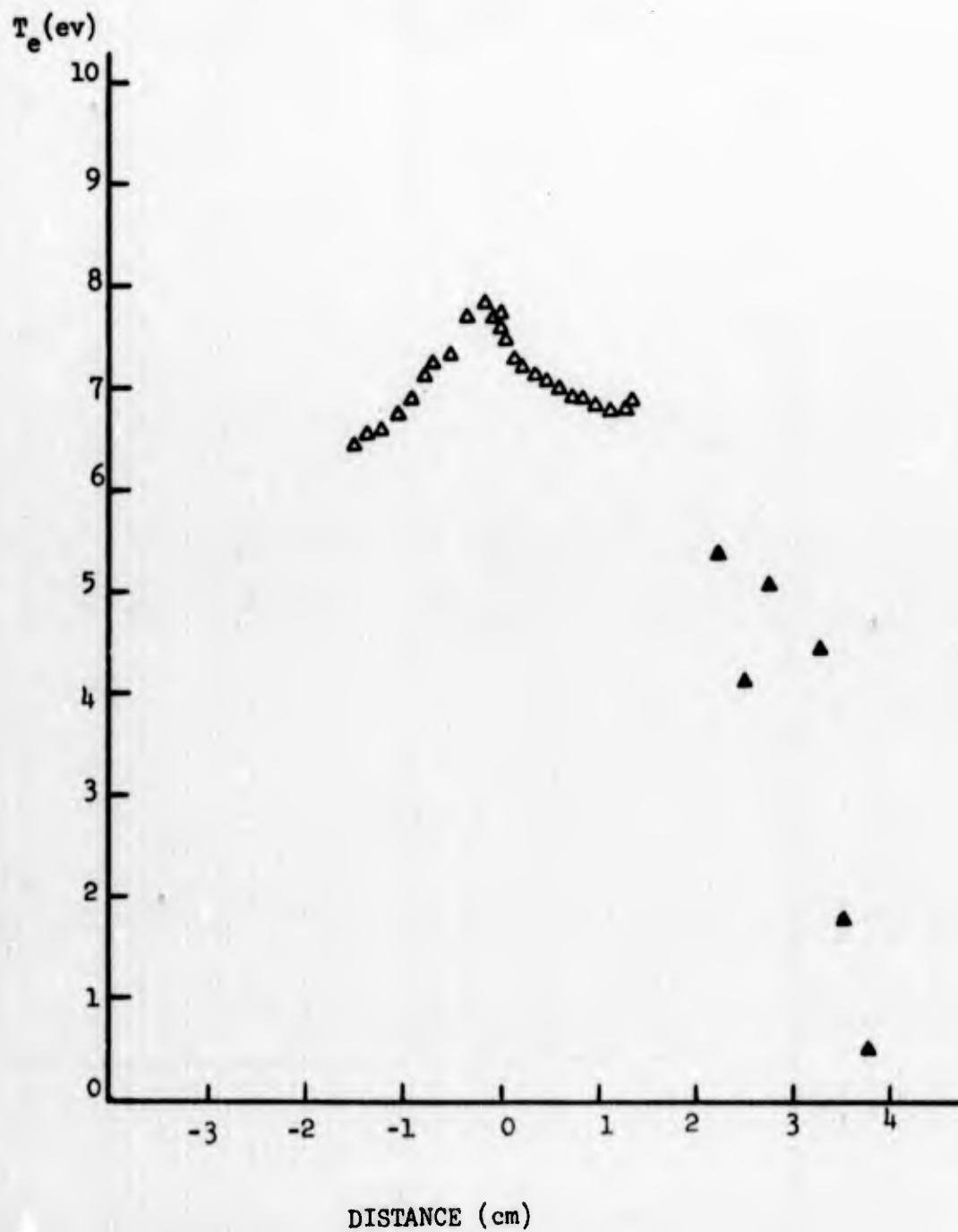


Figure 26 Electron Temperature T_e as Obtained From an IBP and a Langmuir Probe in a Helium Arc

sides of the plasma whereas one Langmuir probe can measure from one side to the core only. Measurements never done before at RPI have been made with some fairly striking results as attested in Figure 24. It is believed that the hollow core of the plasma is caused by the mode of generation and feed of neutral gas, the hollow cathode.

VI. FUTURE CONSIDERATIONS

The development of the IBP is far from finished. There remain many promising areas for improvement and extension of the IBP technique. Undoubtly, after each improvement, a new area will open up, require more improvements and so on. In any case, any improvement will increase the IBP capability of measuring plasma parameters as continuous functions of space and time. The following section outlines two such improvements which are presently under investigation.

A. Slaving System

One definite requirement is put on the IBP system, an absolute knowledge of the magnetic field. Initially this was assumed constant. The beam energy was chosen for a specific B^2/m ratio. This corresponds to a specific set of beam paths that were chosen in the design work. The mass of the ion will not change; isotopes are rare; the speeds of the ions are far from relativistic. The energy of the ion is known to be constant because the power supply is built to be stable, drift free, highly regulated and virtually ripple free. This leaves the magnetic field as a variable. This is known to vary with a period on the order of tens of seconds. The variation is significant enough to alter the beam paths. It is, therefore, necessary to have a unit that actively keeps the system scaled to the proper design orbits. Recently, this unit has been put into operation. This scaling is called slaving. At present, the beam energy and sweep are slaved.

The unit also scales in the different ions. The unit has digital logics that can switch up to three different ions and alter their energy and sweep to maintain the same beam paths. The circuit is shown in Figure 27.

B. Electrostatic Energy Analyzer

The analyzer is the more sensitive detector spoken of earlier. It should be remembered that any detector placed in a plasma environment is constantly bombarded by myriads of charged and neutral particles. In this noisy environment, the desired signal is buried. The analyzer derives its sensitivity by establishing a very definite requirement on the charge, momentum, energy, and origin of the particles.^{24, 25, 26} Particles satisfying the requirements follow paths that intercept a split detector; other particles follow paths that miss the detector and thus are not sampled. There is a noise level caused by particles that do not satisfy the requirements because there is a finite probability for any particle to be scattered to the detector. This noise level is extremely low.

This device has recently been installed on the Rensselaer HCD and is undergoing tests. Signal to noise ratios of 200 to 1 are not uncommon for Potassium ions in an Argon arc. Signals for Sodium, Potassium and Rubidium ions can be detected with little difficulty in both Argon and Helium. This detector will be the subject of a more complete paper at a later date. With the addition of the Electrostatic analyzer, space potential can be measured in addition to temperature and density. A primitive analyzer is shown on Figure 8 for the

measurement of space potential.

C. Future Investigations

As soon as the analyzer is calibrated and its complicated electronics checked, another attempt will be made to compare the IBP with the Langmuir probe. Initial tests show the analyzer to be a much quieter device. It has also been found that the analyzer is a much more sensitive measurer of space potential than density or temperature. Extension to the fringes of the plasma is seen as highly possible.

All the work to this point has been to design, install, and develop an operating IBP on the Rensselaer HCD. This has been the subject of a Ph.D thesis for a student for whom the author of this thesis has served as assistant. The author intends to use the IBP for his Ph.D studies in the investigation of stabilization of coherent instabilities in a plasma. An instability has been detected with the IBP on the Rensselaer HCD. It is the author's intention to study the plasma with and without stabilization with the IBP. It is believed that the ability to make measurements through the entire plasma continuously in space and time should provide some interesting results.

LITERATURE CITED

1. Huddleston, R.H. and Leonard, S.C., Plasma Diagnostic Techniques, (New York 1965).
2. Hickok, R.L., Jobs, F.C. and Marshall, "Spatially Resolved Density Measurements of Deuterium Plasma Using Energetic D⁺ Beam," Review of Scientific Instruments, 37, 5 (1966).
3. Jobs, F.C., Marshall, J.F., and Hickok, R.L., "Plasma Density Measurements by Ion Beam Probing," Phys. Rev. Letters, 22, 20 (1969).
4. Jobs, F.C. and Hickok, R.L., "A Direct Measurement of Plasma Space Potential," Nuclear Fusion, 10 (1970).
5. Hickok, R.L. and Jobs, F.C., "Ion Beam Probe for ST Tokamak," APOSR TR-72-0018, February 1972.
6. Swift, J.D. and Schwar, M.J.R., Electric Probes for Plasma Diagnostics, (London 1966).
7. Huddleston and Leonard, as in (1).
8. Sajben, M., Lee, P.H.Y., "Inverse Problem for Electrostatic Plasma Probes," Journal of Applied Physics, 41, 8 (July 1970), 3433-3439.
9. Langmuir, I., The Collected Works of Irving Langmuir, ed. C. Guy Suits, (New York, 1961), IV, 32-35, 106-118.
10. Bohm, D., Burhop, E.H.S., and Massey, H.S.W., "The Use of Probes for Plasma Exploration in Strong Magnetic Fields," in Characteristics of Electric Discharges in Magnetic Fields, eds. A. Grethrie and R.K. Wakerling, (New York, 1949), 48, 50-57.
11. Langmuir, 106-118, as in (9).
12. Chen, F.F., "Electric Probes," in Plasma Diagnostic Techniques, ed. R.H. Huddleston and S.L. Leonard, (New York 1965), 124.
13. Reinovsky, R., "Ion Beam Probing of High Energy Plasmas," (Ph.D Thesis, Rensselaer Polytechnic Institute, 1973).
14. Kieffer, L.J., Atomic Data, 1, 19 (1969).
15. Reinovsky, as in (13).

16. Hickok, R.L. and Jobes, F.C., Heavy Ion Beam Probe Systems for Plasma Diagnostics, AFOSR 70-2354 TR, December 1970, 5.
17. Kieffer, as in (14).
18. Reinovsky, as in (13).
19. Pierce, J.R., Theory and Design of Electron Beams, (New York, 1949).
20. Tsukkerman, I.I., Electron Optics in Television, translated by Louis Anderson Fenn, (New York 1961).
21. Pierce, as in (19).
22. Stufflebeam, J.H., "Langmuir Probe Measurements in the Presence of a Magnetic Field," (Master's Thesis, Rensselaer Polytechnic Institute, 1970).
23. Reinovsky, as in (13).
24. Harrower, G.A., "Measurement of Electron Energies by Deflection in a Uniform Electric Field," Review of Scientific Instruments, 26, 9 (1955), 850-854.
25. Green, T.S. and Proca, G.A., "A Parallel Plate Electrostatic Spectrograph," Review of Scientific Instruments, 41, 10 (1970), 1409-1414.
26. Proca, G.A. and Green, T.S., "Minimum Image Size in a Parallel Plate Electrostatic Spectrograph," Review of Scientific Instruments, 41, 12 (1970), 1778-1783.

APPENDIX A

Plasma Machine

The plasma source on which the experimental study was taken is a hollow cathode, gas fed, arc discharge. The system is illustrated in Figure 28.

The system consists of a cylindrical primary vacuum vessel 3 meters in length and 15 cm in diameter made of pyrex glass. This vessel is pumped by four 4" oil diffusion pumps that are backed by two 15 cfm mechanical forepumps capable of pressures of the order of one micron. Water baffles, mounted on the intake of the pumps, prevent contamination of the chamber from back-streaming of pump oils. Gate valves, located above the water baffles, allow variation of the pumping speed from zero to the maximum of twenty-two hundred liters per second.

The pumping chamber is immersed in a magnetic field produced by 6 water cooled Magnion 12" ID air core coils. Power is delivered to the magnets through a buss system allowing interconnection of up to 4 high current DC supplies. In this way, the confining field can be operated in a variety of uniform or mirror type configurations. Maximum field strengths are of the order of 3000 gauss.

The primary vacuum cylinder was modified to allow for the IBP installation by the construction of a 60 cm x 100 cm rectangular chamber to fit between 2 magnetic coils as seen in Figure 28. This chamber has conductance-limiting baffles separating it from the

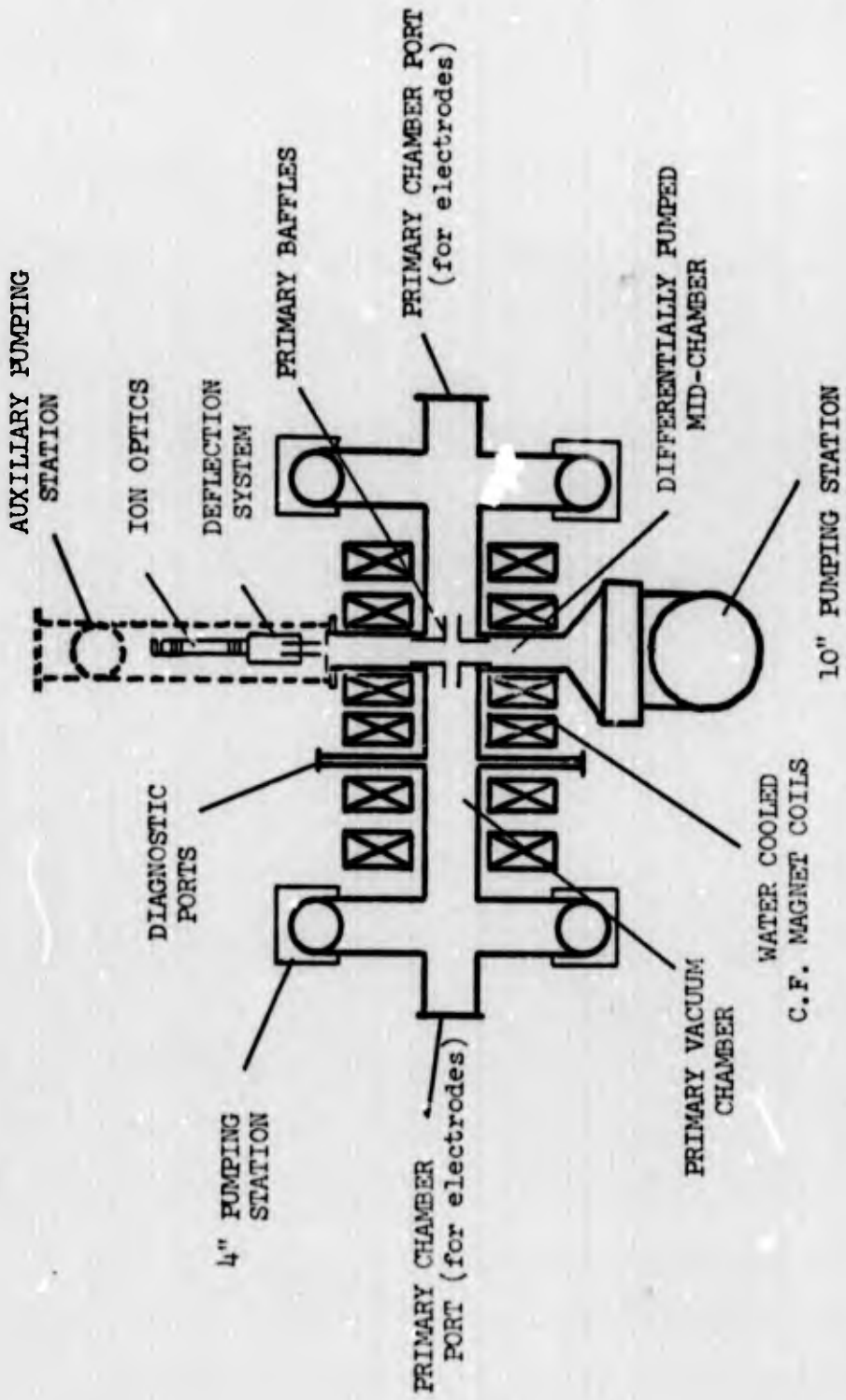


Figure 28 RPI Plasma Machine

primary chamber and is differentially pumped using a 10" oil diffusion pump. This pump is opened or closed to the system by means of a 10" pneumatically operated gate valve. The top and one side of the chamber are provided with numerous access ports for beam probing and other diagnostics.

All foreline pumping is interconnected with 2" copper pipe. One mechanical pump backs up the 10" pump; the other backs up the four 4" pumps. Sections of foreline can be made isolated or connected to the system by means of 2" pneumatically operated gate valves. To bring the system down from atmosphere, a 30 cfm mechanical pump is used to rough the primary vacuum vessel and the reaction chamber. This pump handles the high pressure well and quickly brings the system to around 100 microns where the oil diffusion pumps can be opened to the system.

A third portable pumping station differentially pumps the region housing the electrostatic ion gun for the beam probe. This station is essentially independent of the rest of the system and is used when background pressures are too high in the vicinity of the high voltage gun structure.

Pressure is measured by a Veeco RG-75P ionization gauge. There are four gauges on the system. Two are located at the electrode ports, one is located above the 10" pump, and the fourth is located on the auxiliary pumping station. Because of the variety of conditions in which the system may operate, a control-interlock system was designed and installed to protect the vacuum equipment.

The length of the discharge is adjustable by movement of either water cooled electrode up to 35 cm. This provides for a maximum discharge length of 75 cm and a minimum length of less than 1 cm.

The hollow cathode is a cylinder of bariated tungsten two inches long pushed into the copper tip of the electrode. The copper tip is threaded to fit into a stainless steel tube, forty inches long which supports the whole assembly. Various inner diameter cathodes are available ranging from one-eighth to one-half inch, with a wall thickness of 0.1 in. A small disc of boron nitride is used to shield the copper and stainless steel from the discharge. The anode assembly is the same as the cathode with two exceptions. In both cases, no bariated tungsten is used. For one mode, a flat plate forms the anode; the disc of boron nitride shields just the stainless steel, allowing the exposed copper tip to act as an anode. The other configuration is a hollow anode with an inside diameter of $3/4$ ". This structure is made of copper pipe and is wrapped with copper tubing for water cooling. All electrode structures are water cooled; the hollow anode is the most efficiently cooled. All electrode structures have provisions for feeding gas through them into the chamber.

The voltage and current required to maintain the arc are supplied from a Miller DC welding supply providing an open circuit voltage of 140 volts. The initial breakdown of the gas is accomplished with an r-f generator which is momentarily connected in parallel with the DC welding supplies.

Diagnostics of the discharge are obtained primarily through the use of Langmuir probes and the Ion Beam Probe. Spectrographic and laser scattering methods are being developed.

The plasma machine can operate in 3 modes of operation. The first mode is the hollow cathode flat anode. The second is the hollow cathode, hollow anode; this mode features higher current, higher background pressure and presumably better gas utilization. The third mode is established by removing the DC electrodes and installing a microwave structure similar to those described by Lisitano, producing a microwave-induced electron resonance plasma, MIERP. Switching from mode to mode is accomplished in one hour. In addition to the three modes, two gases are commonly used: Argon and Helium.

With the described plasma machine, the following operating characteristics are observed.

Arc Current	20 - 35 amps
Arc Voltage	20 - 75 volts
Magnetic Field	500 - 2000 gauss
Pressure	10^{-4} - 10^{-3} torr
Electron Temperature	10 - 20 eV (in core) 1 - 2 eV (outside)
Ion Temperature	0.1 - 0.5 eV
Gas Temperature	0.1 eV
Charged Particle Density	10^{13} cm^{-3} - 10^{14} cm^{-3} (in core) 10^{10} cm^{-3} - 10^{12} cm^{-3} (outside)

APPENDIX B

```

100 ALPHA FUNC,BB,INFILE,IIILE(10,5)
103 FILENAME FILE
109 INTEGER CH,POW
114 REAL USAL,LENP,M,K
119C
122C
129 DATA BB/"B"/
134C
133C
140 READ ("AUXFILE", 902) INFILE, I
141 I = 1/6.025E26
145 READ ("AUXFILE", 903) IIILE
150 READ ("AUXFILE", 904) USCAL, ASCAL, RADP, LEMP
155 FILE = INFILE
160 PRINT 905, IIILE
165 PRINT 906, RADP, LEMP
170 E = 1.60210E-19
175 K = 1.33054E-23
180 RADP = RADP*2.54E-5
185 LEMP = LEMP*0.01
300 READ(FILE, 901) CH, FUNC, DGIS, POW
310 IF(CH.NE.1) STOP
320 200 IF (FUNC.EQ.BB) DGIS = -DGIS
330 RADIUS = DGIS/10**POW
340C
341C INITIALIZE SUMS
342C
350 SUMXI = 0
360 SUMYI = 0
370 SUMXY = 0
380 SUMX2 = 0
390 SUMY2 = 0
400 N = 0
405 LEAP = 0
410 10 N = N + 1
420 READ (FILE, 901, END = 1000) CH, FUNC, DGIS, POW
430 IF (CH.EQ.1) GO TO 200
435 IF (CH.NE.2) STOP
440 IF (FUNC.EQ.BB) DGIS = -DGIS
450 X = DGIS*USCAL/10**POW
460 READ (FILE,901) CH, FUNC, DGIS, POW
470 IF(CH.NE.3) STOP
480 IF(FUNC.EQ.BB) DGIS = -DGIS
490 Y = DGIS*ASCAL/10**POW
500 IF(IFAP.EQ.1) GO TO 101
510 SUMXI = SUMXI + X
520 SUMYI = SUMYI + Y
530 SUMXY = SUMXY + X*Y
540 SUMX2 = SUMX2 + X*X
550 SUMY2 = SUMY2 + Y*Y

```

```

560 IF(N.EQ.1) GO TO 12
570 ISAI = -Y
580 GO TO 10
590 12 10P = N*SUMXY - SUMXI*SUMYI
600 B01 = N*SUMX2 - SUMXI*SUMXI
610 SLOPE = 10P/B01
615 B = (SUMYI/N) - SLOPE*SUMXI/N
620 DEVNEW = SUMY2 - (B*SUMYI + SLOPE*SUMXY)
630 IF(N.EQ.2) GO TO 13
640 IF (DEVNEW .GT. DEVOLD .AND. N .GT. 10) GO TO 20
650 13 DEVOLD = DEVNEW
660 30 10 10
670C
680 20 1EXP = 1
690 PRINT 907, RADIUS, SLOPE, B, N, DEVNEW
691 SLLIN = SLOPE
692 BLIN = B
700 N = N - 1; L = 0
710 SUMXI = 0
720 SUMYI = 0
730 SUMXY = 0
740 SUMX2 = 0
750 SUMY2 = 0
760 101 Y = Y - (SLLIN*X + BLIN)
770 IF(Y.GT. 0.00) GO TO 102
780 N = N - 1; GO TO 10
790 102 Y = ALOG(Y)
800 SUMXI = SUMXI + X
810 SUMYI = SUMYI + Y
820 SUMXY = SUMXY + X*Y
830 SUMX2 = SUMX2 + X*X
840 SUMY2 = SUMY2 + Y*Y
850 IF(N.EQ. 1) GO TO 10
860 10P = N*SUMXY - SUMXI*SUMYI
870 B01 = N*SUMX2 - SUMXI*SUMXI
880 SLOPE = 10P/B01
885 B = (SUMYI/N) - SLOPE*SUMXI/N
890 DEVNEW = SUMY2 - (B*SUMYI + SLOPE*SUMXY)
910 I = E/(X*SLOPE)
920 DENS = SURF((3.14159*N)/(2*(K+1)))*(ISAI/(E*3.14159*RADP*LENP))
930 I = I*.17E4
940 DENS = DENS/1.00E6
950 IF(N.LI.(L + 3)) GO TO 10
960 L = N
970 PRINT 908, N, I, DENS, DEVNEW
980 GO TO 10
990 901 FORMAT (4X, I2, A1, F6.0, I1)
1000 902 FORMAT (4X, A4, 2X, E10.0)
1010 903 FORMAT (4X, 10A4)
1020 904 FORMAT ( 4X, 4E10.4)

```

```
1030 905 FORMAT (" ", "LANGMUIR PROBE DATA"// (4X, F10.2))
1040 906 FORMAT (///" ", "PROBE RADII IS ", F4.1, " MILS")
1041&    " ", "PROBE LENGTH", F4.3, " CM.")
1050 907 FORMAT (" ", 5X, "PROBE AT RADII", F4.3//
1051&    " ", "10V SATURATION REGION DEFINED BY"
1052&    " ", 5X, "AMPS = ", 1P59.2, " * VOLTS + ", F10.2/
1053&    " ", 5X, "LINEAR FIT USED ", 1P, " POINTS, WITH DEVIATION", F10.2
1055&    " ", "EXPONENTIAL REGION"
1056&    9X, "TEMP", 4X, "DENSITY", 3X, "DEVIATION")
1060 908 FORMAT (15, F10.3, 1P2E10.2)
1070 1000 STOP
1080 END
```

PROBE

```

10 LET E=1.6E-19
20 LET K=1.33E-23
30 LET M=6.67E-26
40 PRINT "THE GAS USED IS ARGON"
50 LET R1=1.3E-04
60 LET L=.004
70 READ G,J
80 LET D=1
90 READ F1,F2,B,I,V
100 LET D=D+1
110 LET B1=4.45*B
120 PRINT
130 PRINT
140 PRINT
150 PRINT TAB(20); "THE MAGNETIC FIELD IS"; B1; "GAUSS"
160 PRINT
170 PRINT TAB(14); "THE ARC CURRENT AND VOLTAGE ARE"; I;"AMPS";
180 PRINT V;"VOLTS"
190 PRINT TAB(23); "CATHODE FLOW RATE IS"; F1
200 PRINT TAB(24); "ANODE FLOW RATE IS"; F2
210 PRINT
220 PRINT
230 PRINT
240 PRINT TAB(6); "R"; TAB(16); "ELECTRON TEMP."; TAB(42);
250 PRINT "ION DENSITY"; TAB(53); "VF"; TAB(63); "VS"
260 PRINT TAB(5); "CM"; TAB(14); "(DES K)"; TAB(31); "(EV)";
270 PRINT TAB(42); "(PER CU. CM)"; TAB(56); "(VOLTS)"; TAB(65);
280 PRINT "(VOLTS)"
290 PRINT
300 PRINT
310 LET C=1
320 READ R
330 LET C=C+1
340 FOR X=1 TO 3
350 READ H(X),K(X)
360 LET H(X)=H(X)/1000
370 NEXT X
380 FOR Y=1 TO 2
390 LET T(Y)=(E/K)*(K(Y)-K(Y+1))/LOG(H(Y)/H(Y+1))
400 NEXT Y
410 LET T(3)=(E/K)*(K(1)-K(3))/LOG(H(1)/H(3))
420 FOR W=1 TO 3
430 LET S(W)=T(W)/1.17E04
440 NEXT W
450 LET T1=(T(1)+T(2)+T(3))/3
460 LET I2=T1/1.17E04
470 READ I2,V2
480 LET I2=I2/1000
490 FOR Z=1 TO 3
500 LET N(Z)=SOR((3.14159*M)/(2*(PI(Z)))*(I2/(E*3.14*R1*L))

```

```
510 NEXT Z
520 LET N1=(N(1)+N(2)+N(3))/3
530 LET N1=N1/1.0E06
540 LET V3=V2+4.94*T1/1/17E04
550 PRINT TAB(4); R; TAB(15); T1; TAB(23); T2; TAB(42); N1;
560 PRINT TAB(56); V2; TAB(64); V3
570 IF C<=G THEN 320
580 IF D<=J THEN 90
600 DATA 3,1
601 DATA 5.4,1.2,370,13,45
602 DATA .5,16,-5,1,-7.5,.5,-10,50,-6.5
603 DATA 1,7.5,0,3,-2.5,2,-5,15,-.7
604 DATA 1.5,2.87,2.5,1.75,1.25,1.12,0,13.5,3.3
999 END
```